CHEMBIOCHEM

Supporting Information

Formaldehyde as a Chemical Defence Agent of Fruiting Bodies of *Mycena rosea* and its Role in the Generation of the Alkaloid Mycenarubin C

Rieke Himstedt,[a] Silke Wagner,[a] Robert J. R. Jaeger,[a] Michèle-Laure Lieunang Watat,[a] Jana Backenköhler,[a] Zeljka Rupcic,[b] Marc Stadler,[b] and Peter Spiteller*[a]

cbic_201900733_sm_miscellaneous_information.pdf

Supporting Information

Formaldehyde as a Chemical Defence Agent of Fruiting Bodies of *Mycena rosea* and its Role in the Generation of the Alkaloid Mycenarubin C

*Rieke Himstedt,[a] Silke Wagner,[a] Robert J. R. Jaeger,[a] Jana Backenköhler,[a] Michèle-Laure Lieunang Watat,[a] Zeljka Rupcic,[b] Marc Stadler,[b] and Peter Spiteller[a]**

[a] *Institut für Organische und Analytische Chemie, Universität Bremen, Leobener Straße 7, 28359 Bremen, Germany*

[b] *Mikrobielle Wirkstoffe, Helmholtz-Zentrum für Infektionsforschung, Inhoffenstraße 7, 38124 Braunschweig, Germany*

Structures of Selected Compounds

Selected Mycenarubins Present in *Mycena* Species

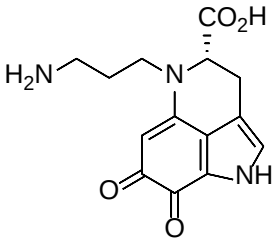

1

Mycenarubin A (**1**)

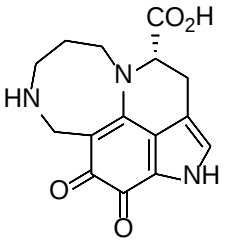

2

Mycenarubin C (**2**)

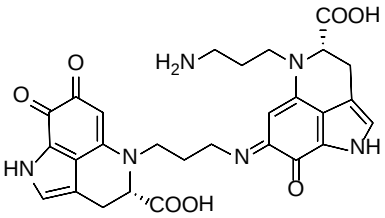

3

Mycenarubin B (**3**)

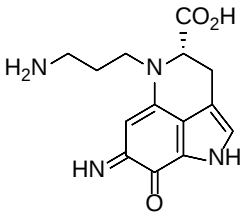

4

Mycenarubin D (**4**)

Compounds Used for the Quantification of Formaldehyde in Mushrooms

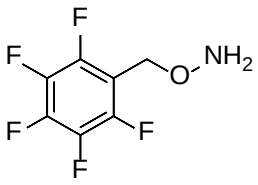

5

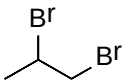

6

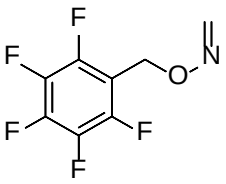

7

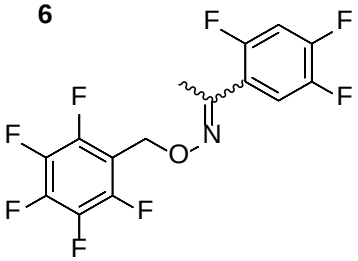

8
($E^{-}{}^{+}Z^{-}$)

Table of Contents

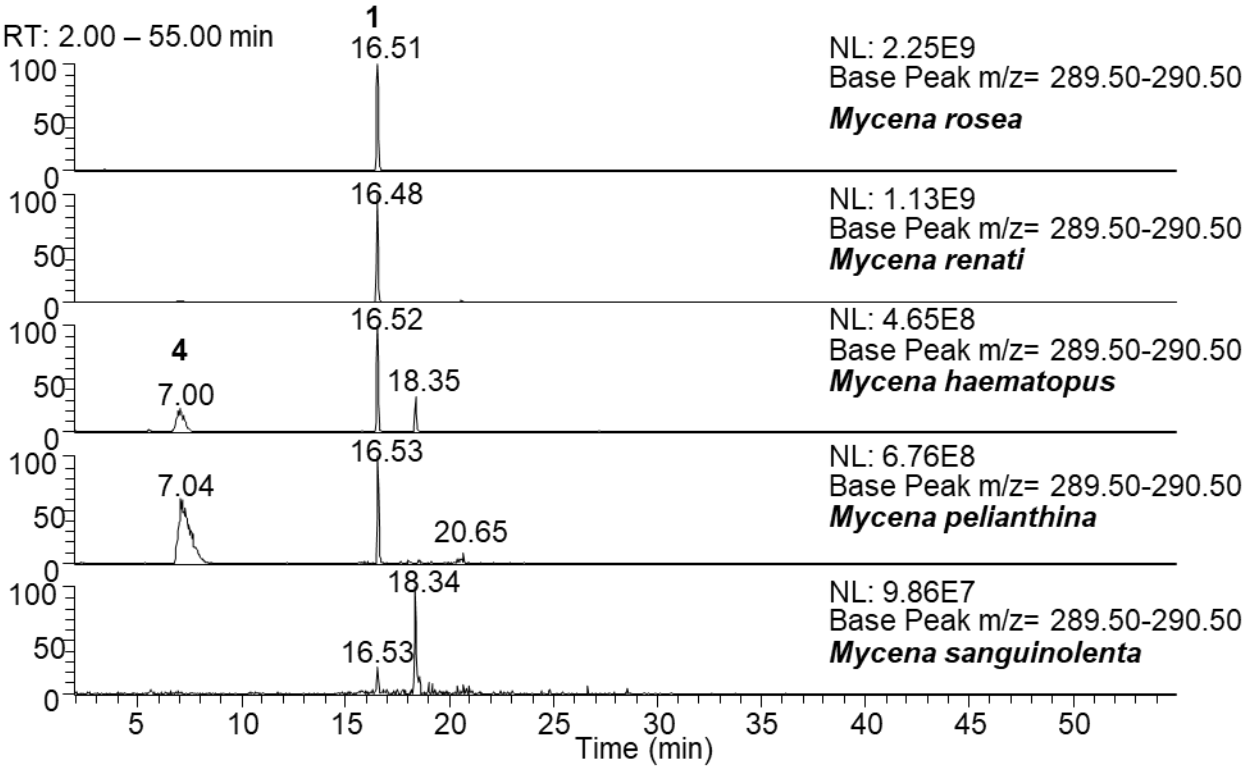

Figure S1. Extracted Ion Chromatograms at *m/z* 290 of the LC-(+)-ESI-MS spectra obtained from crude extracts of different *Mycena* species. Mycenarubin A (**1**) occurs at a retention time of 16.5 min in all shown species. Mycenarubin D (**4**) occurs at 7.0 min and is present in *M. haematopus* and *M. pelianthina*.[S1]

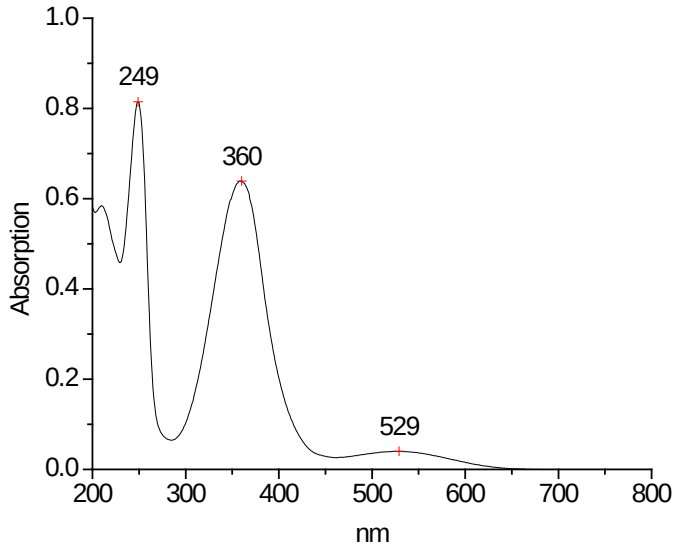

Figure S2. UV/Vis spectrum of mycenarubin C (**2**) in H_2O.

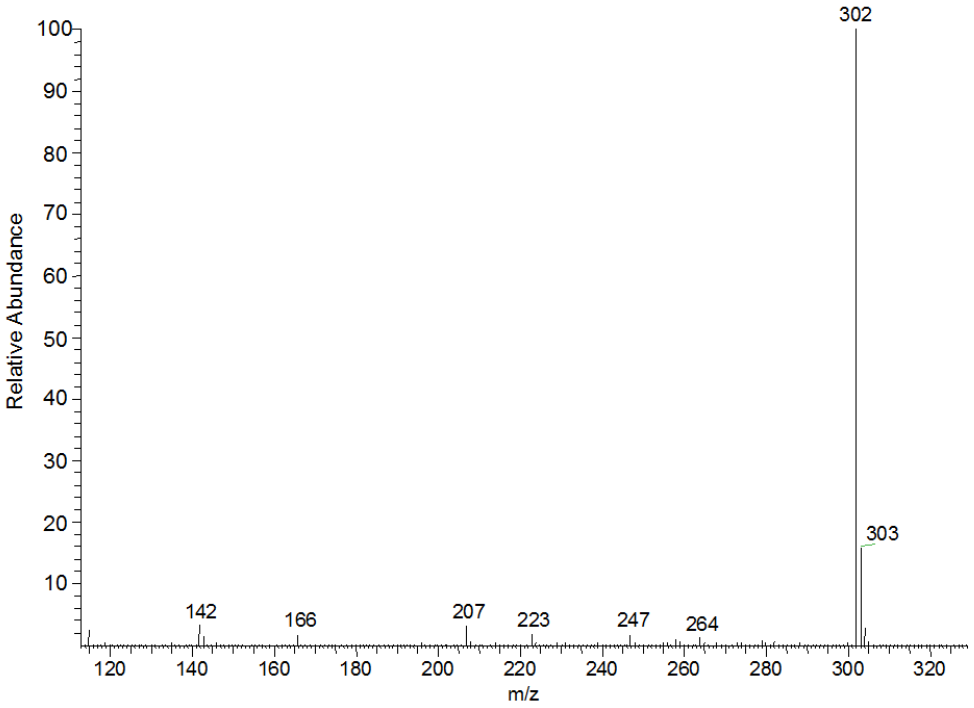

Figure S3. LC-(+)-ESI-MS spectrum of mycenarubin C (**2**).

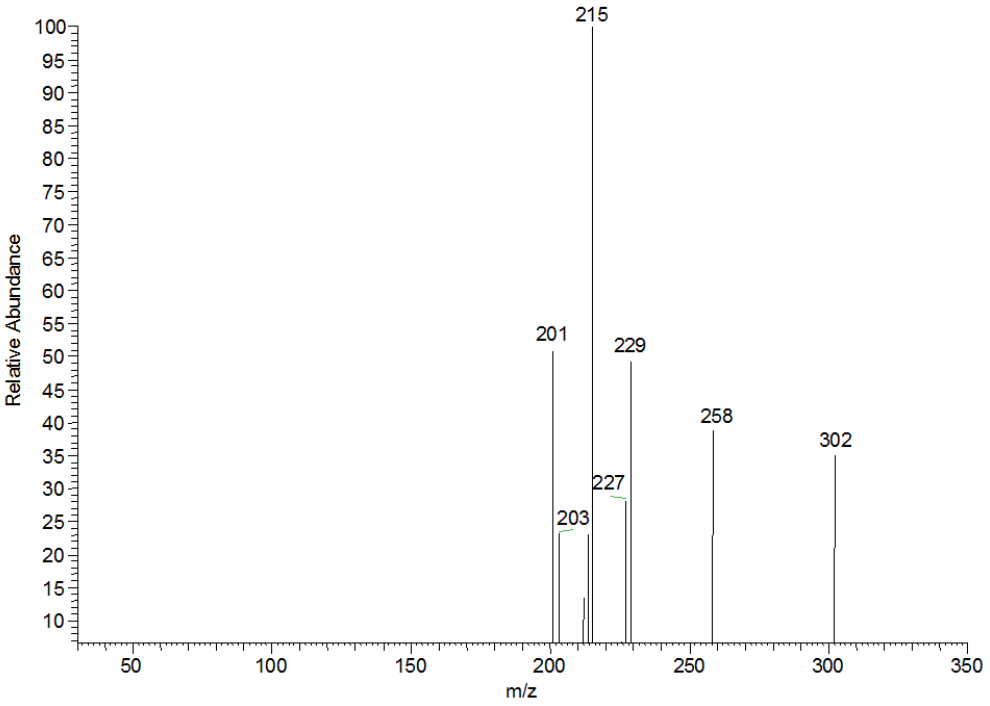

Figure S4. LC-(+)-ESI-MS/MS spectrum (precursor ion *m/z* 302, 25 eV) of mycenarubin C (**2**).

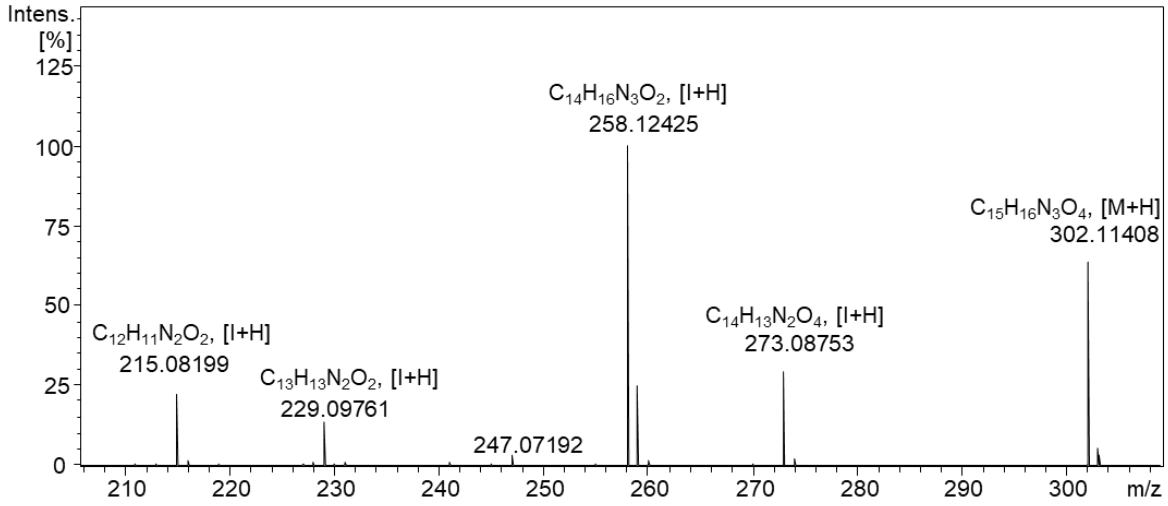

Figure S5. HR-(+)-ESI-MS/MS spectrum (precursor ion *m/z* 302.11408, 15 eV) of mycenarubin C (**2**).

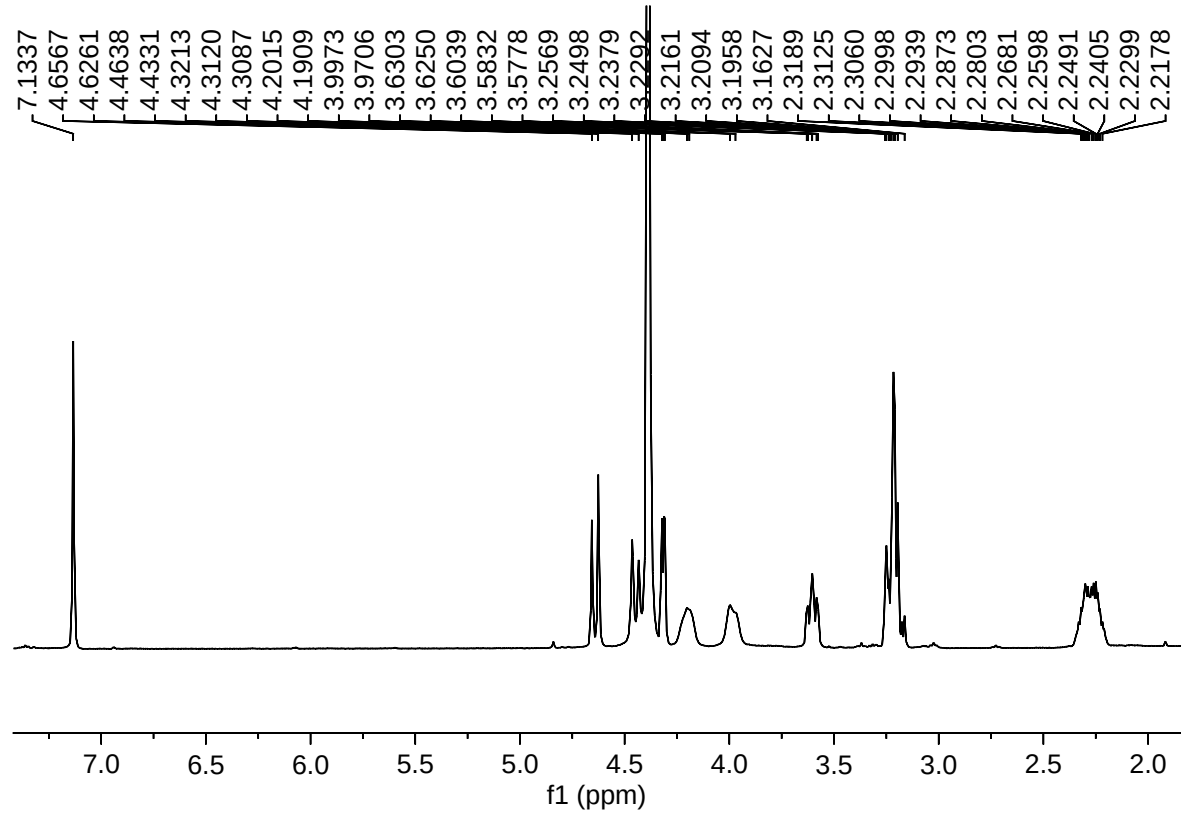

Figure S6. ^{1}H NMR spectrum (500 MHz, D_2O, 335 K) of mycenarubin C (**2**).

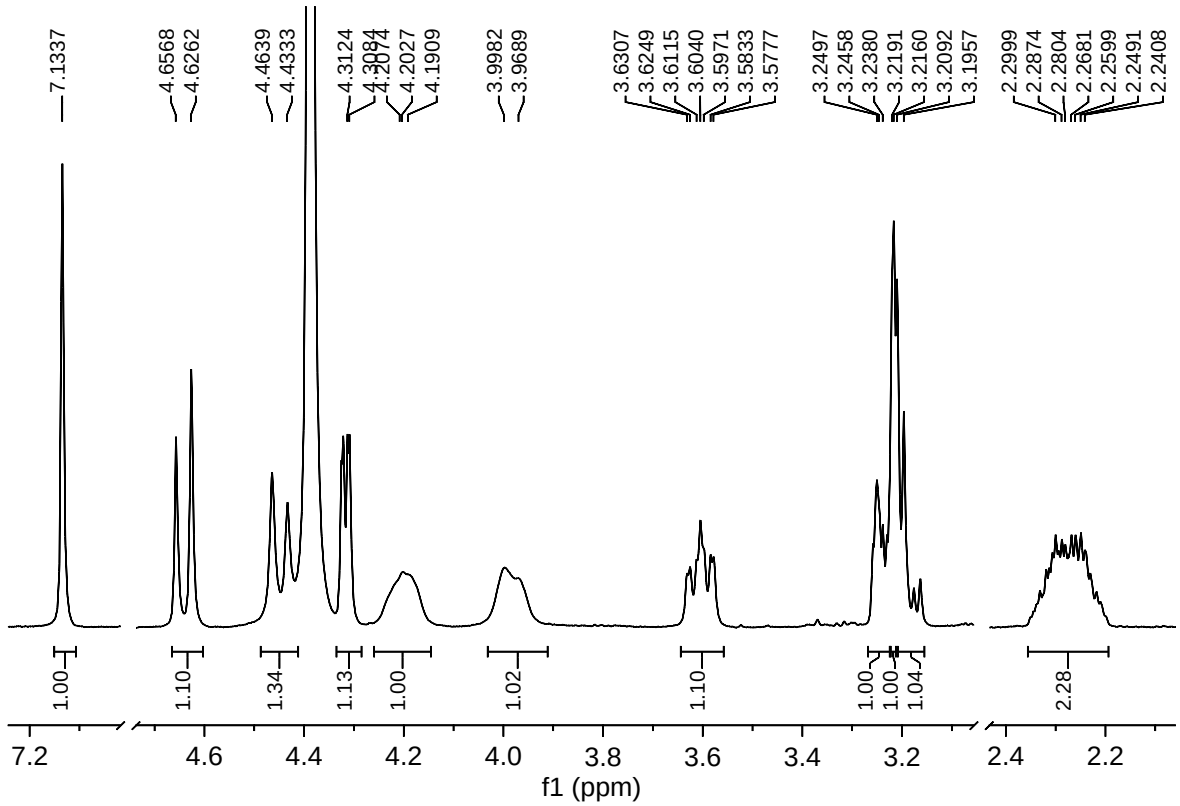

Figure S7. ^{1}H NMR spectrum (500 MHz, D_2O, 335 K) of **2**. Signal-free areas are removed.

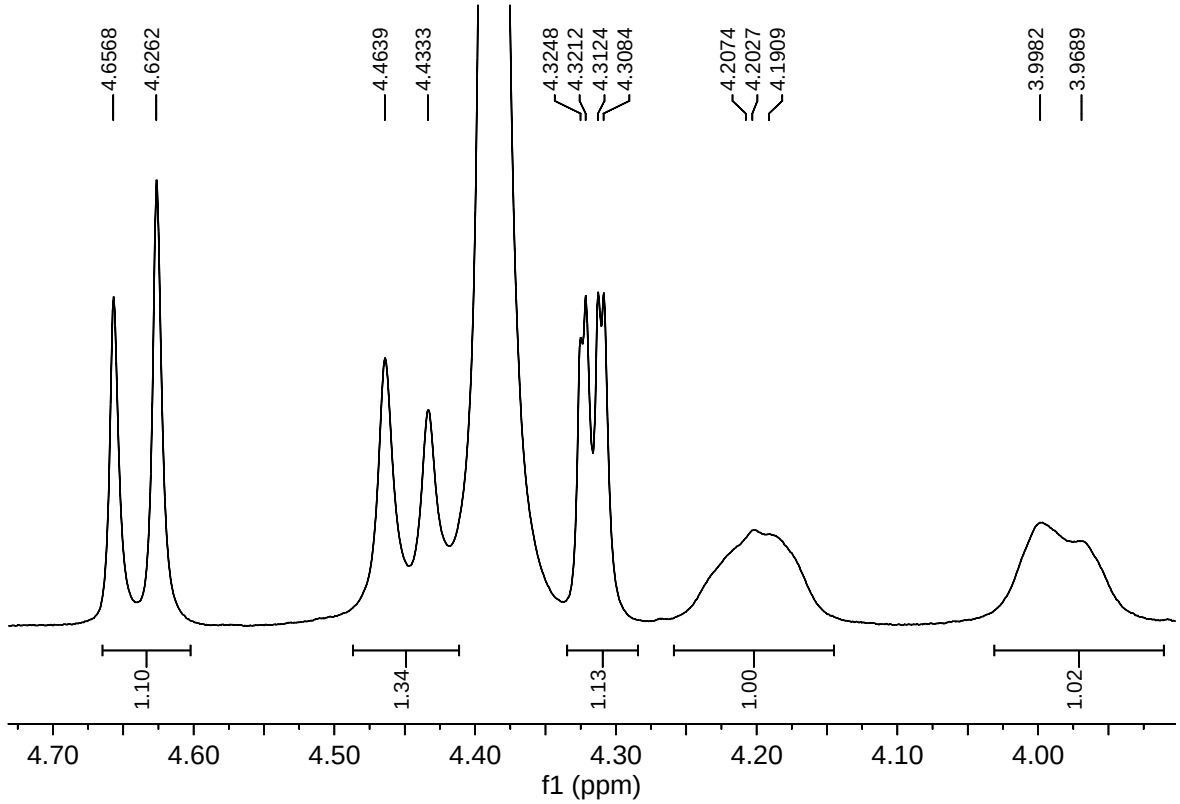

Figure S8. ^{1}H NMR spectrum (500 MHz, D_2O, 335 K, range: 3.8 – 4.8 ppm) of **2**.

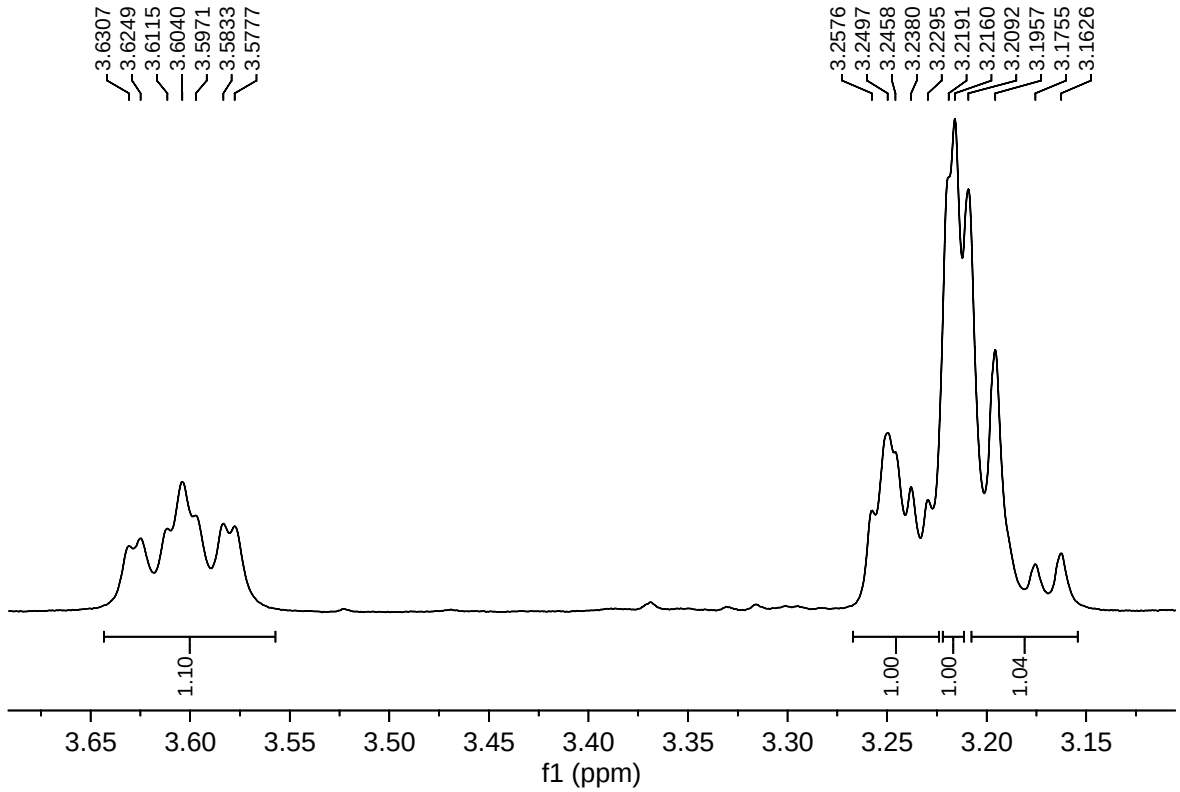

Figure S9. ^{1}H NMR spectrum (500 MHz, D_2O, 335 K, range: 3.1 – 3.7 ppm) of **2**.

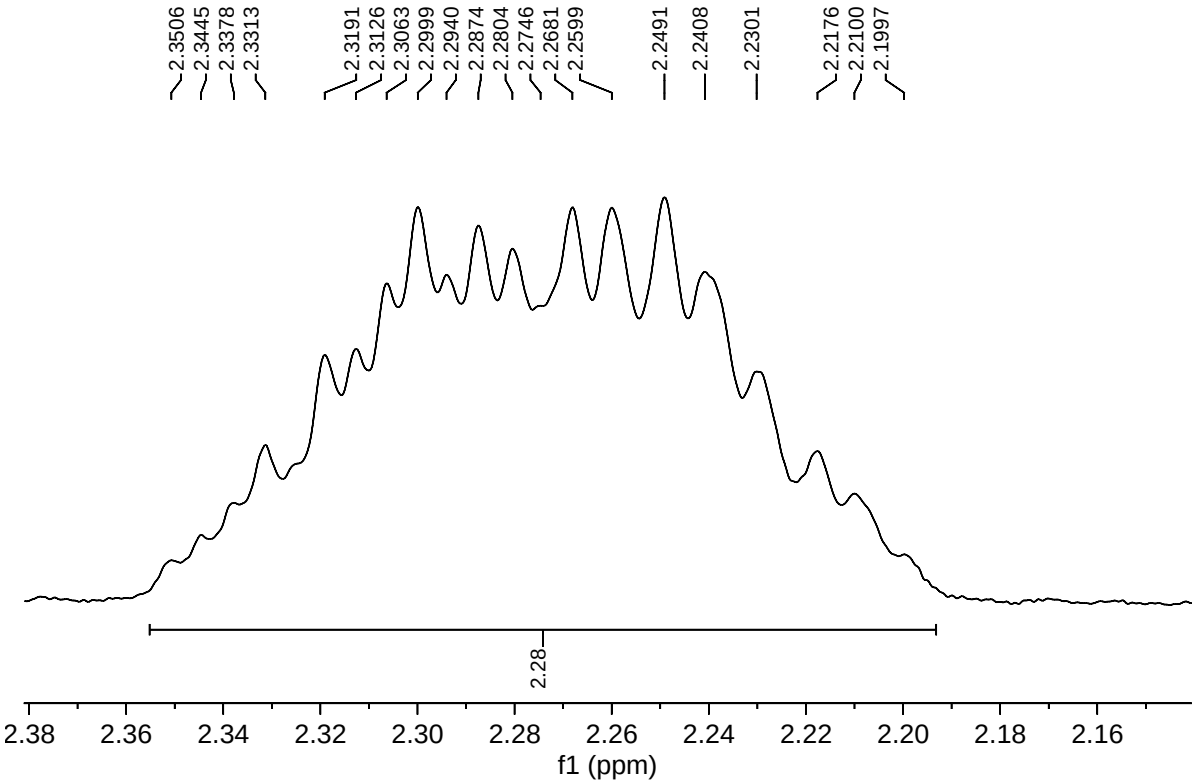

Figure S10. ^{1}H NMR spectrum (500 MHz, D_2O, 335 K, range: 2.14 – 2.38 ppm) of **2**.

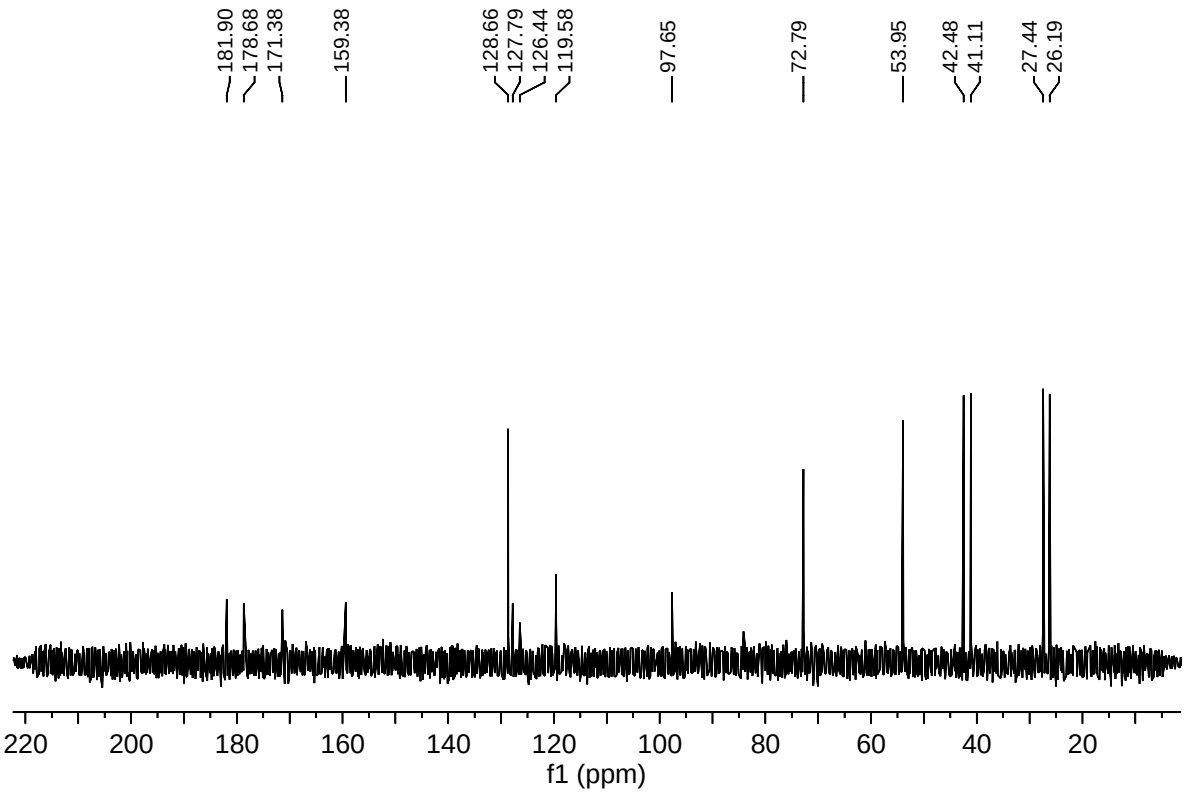

Figure S11. ^{13}C NMR spectrum (151 MHz, D_2O, 330 K) of **2**.

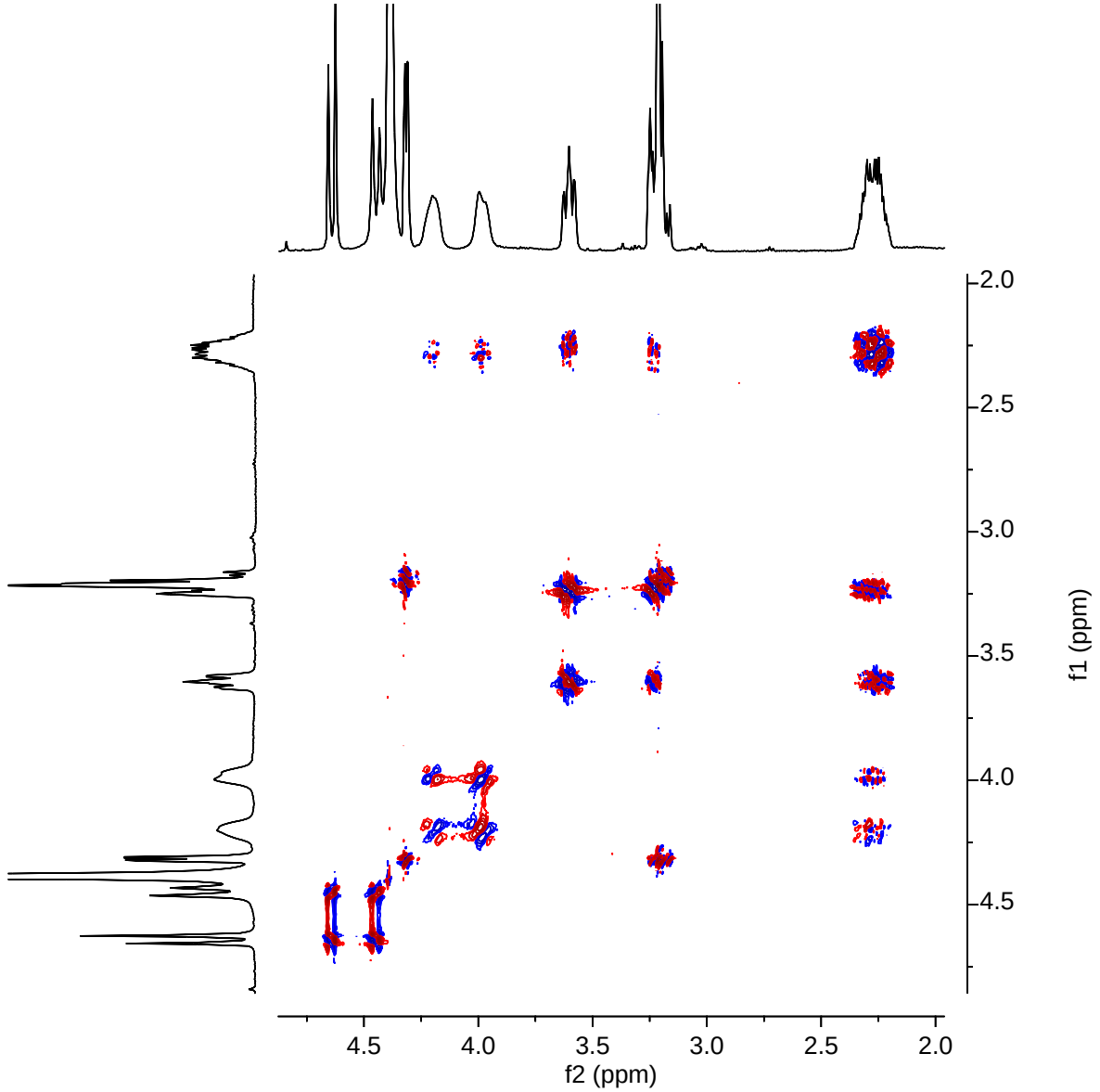

Figure S12. COSY (500 MHz, D_2O, 335 K) of **2**.

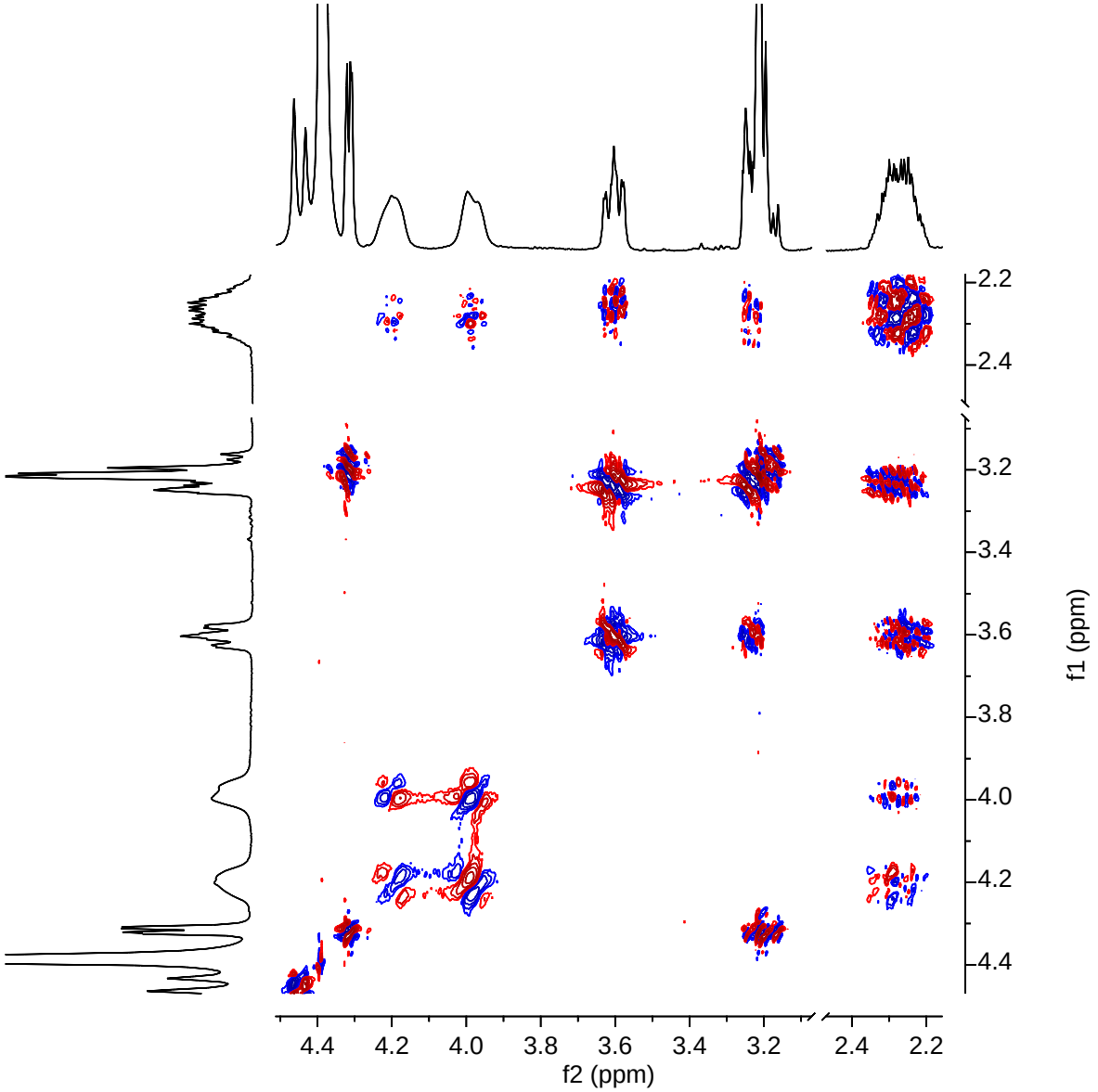

Figure S13. COSY (500 MHz, D_2O, 335 K, range 2.2 – 4.4 ppm) of **2**. Signal-free areas are removed.

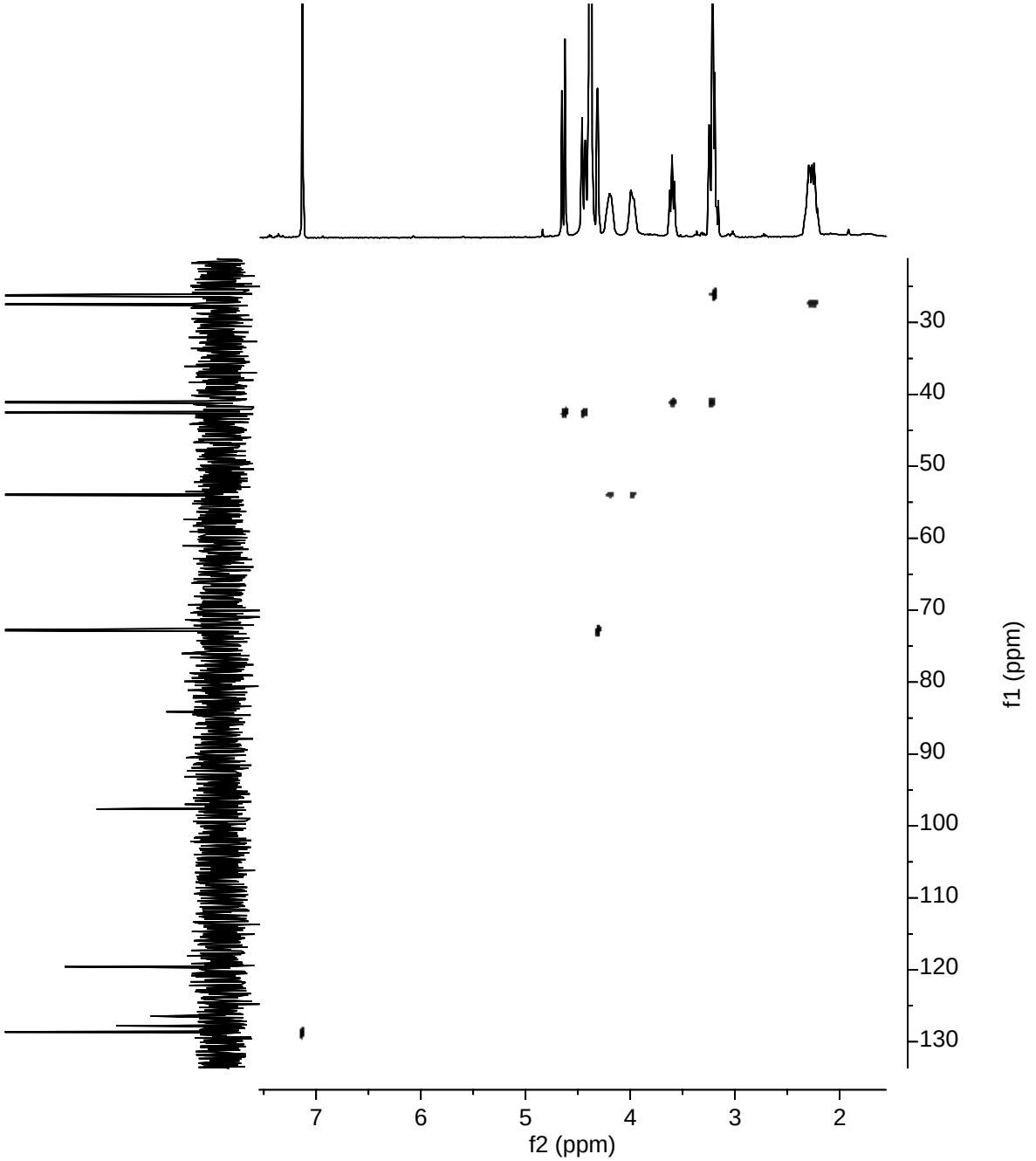

Figure S14. HSQC (500 MHz, D_2O, 335 K) of **2**.

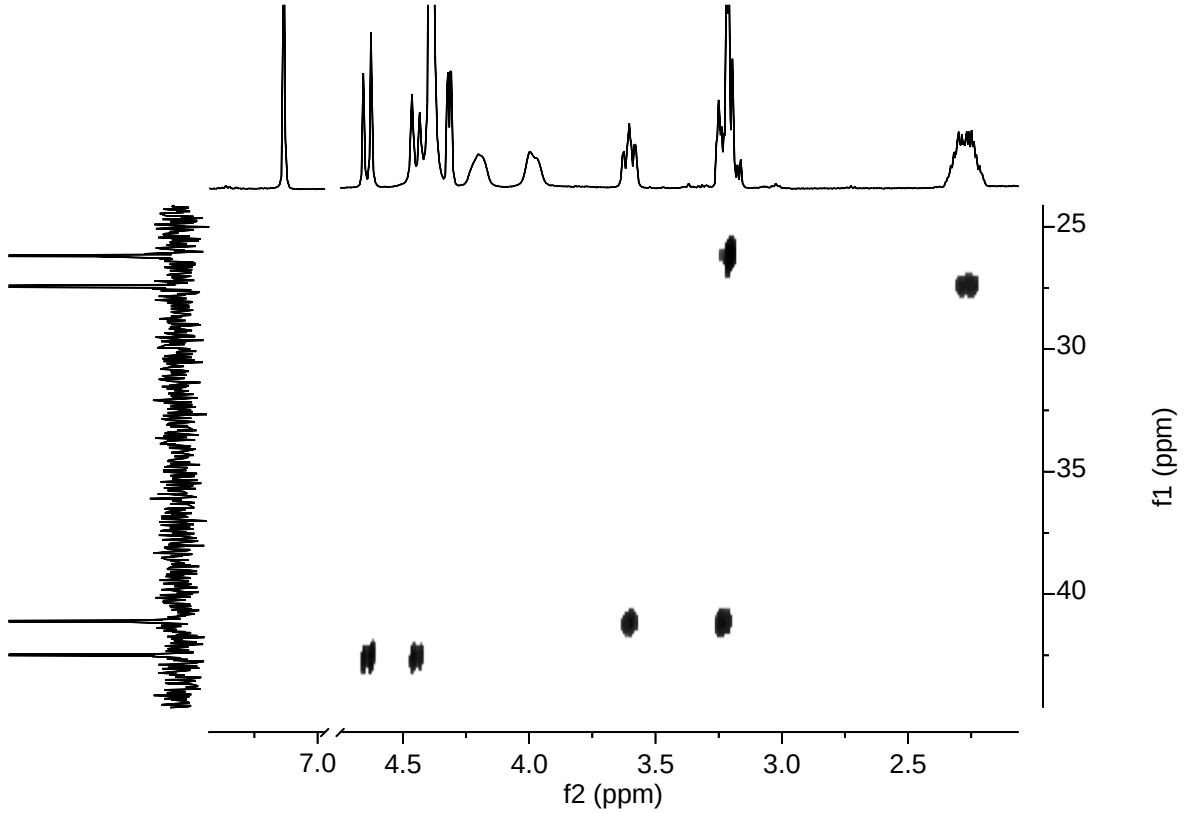

Figure S15. HSQC (500 MHz, D_2O, 335 K, f1 range 25 – 45 ppm) of **2**. Signal-free areas removed.

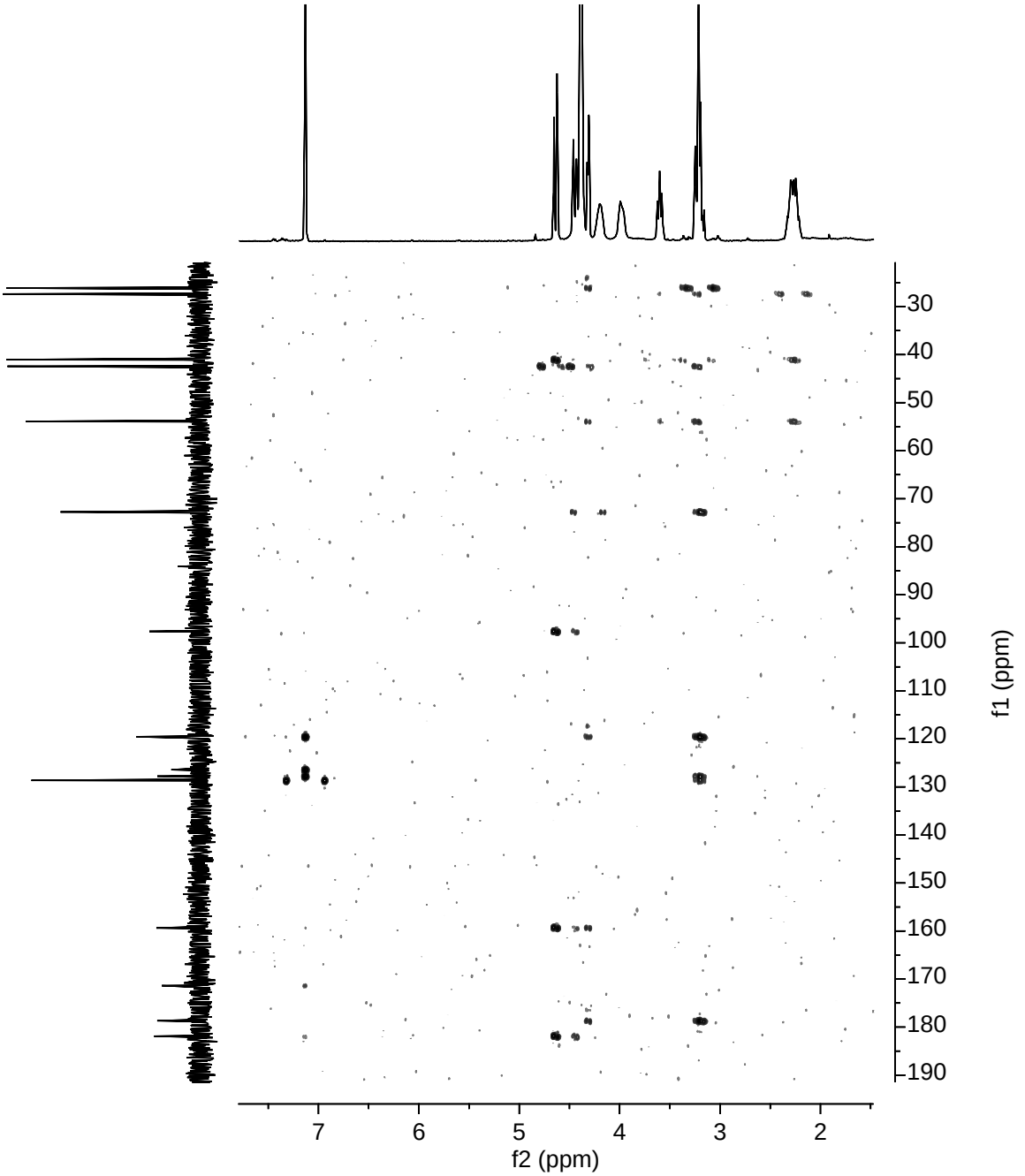

Figure S16. HMBC of **2** (500 MHz, D_2O, 335 K).

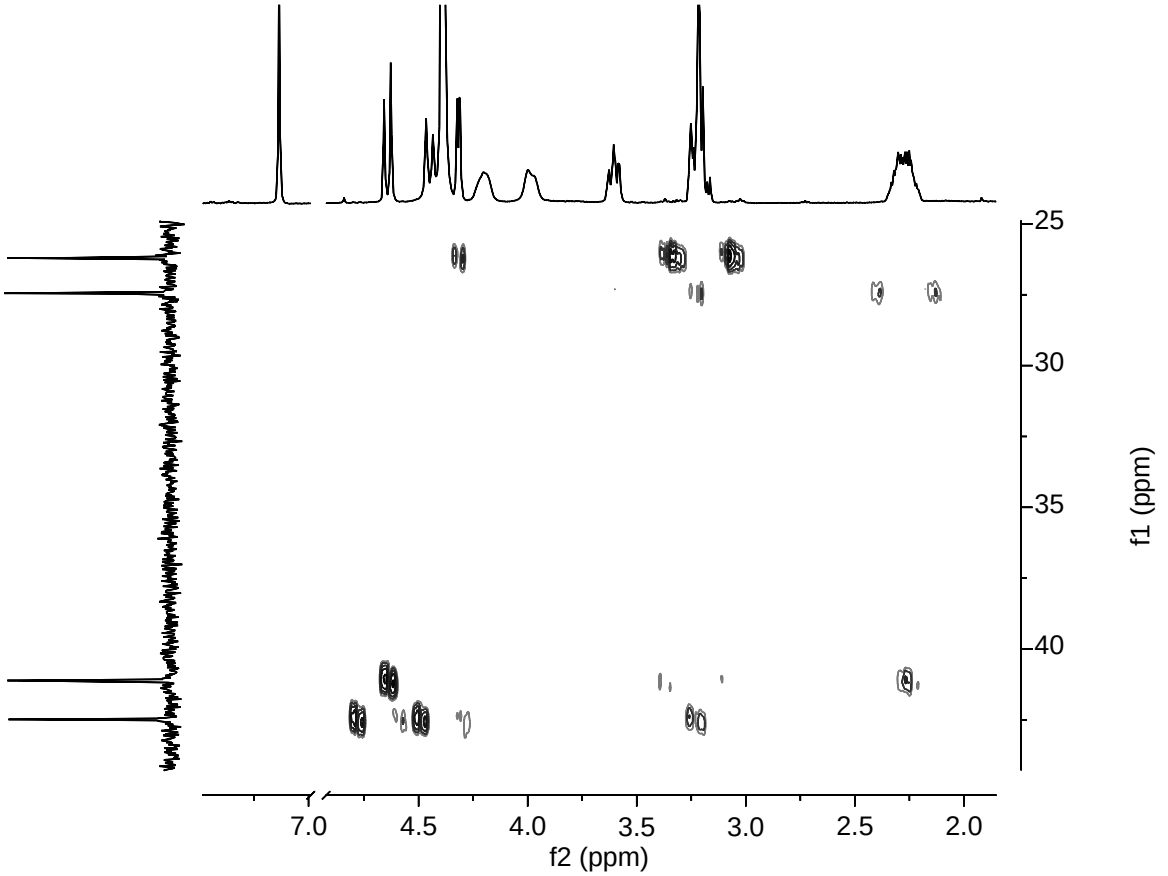

Figure S17. HMBC of **2** (500 MHz, D_2O, 335 K, f1 range 25 – 45 ppm). Signal-free areas removed.

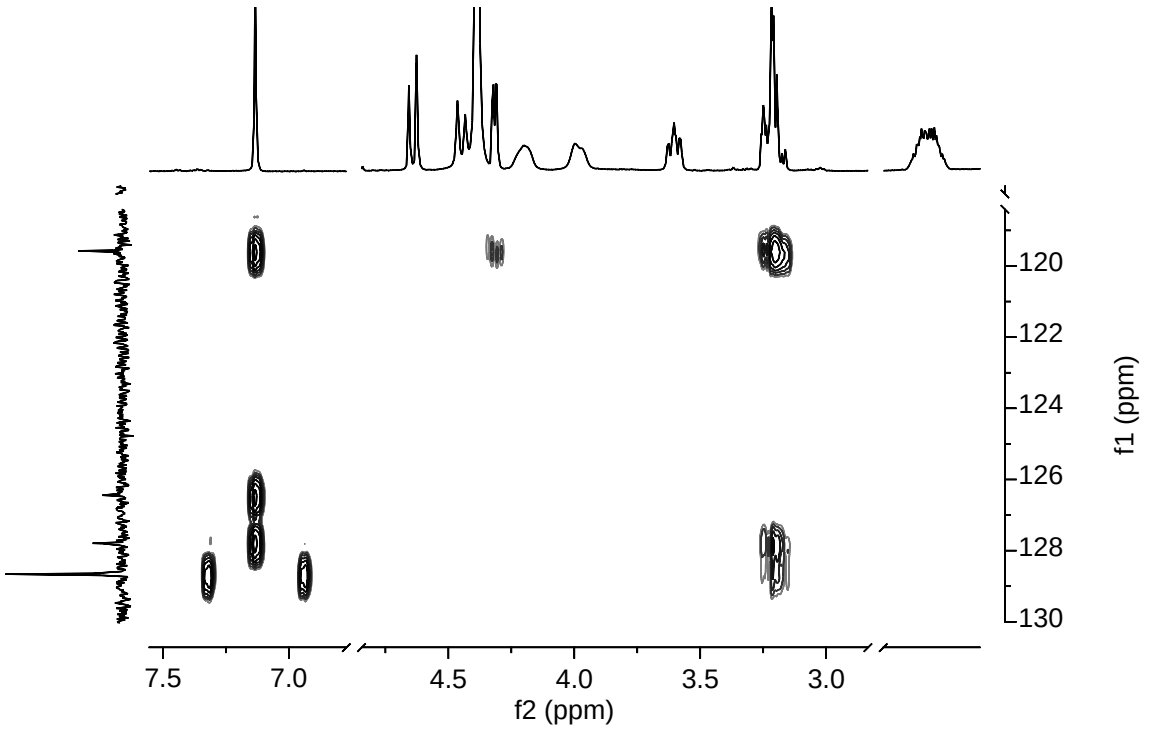

Figure S18. HMBC of **2** (500 MHz, D_2O, 335 K, f1 range 119 – 130 ppm). Signal-free areas removed.

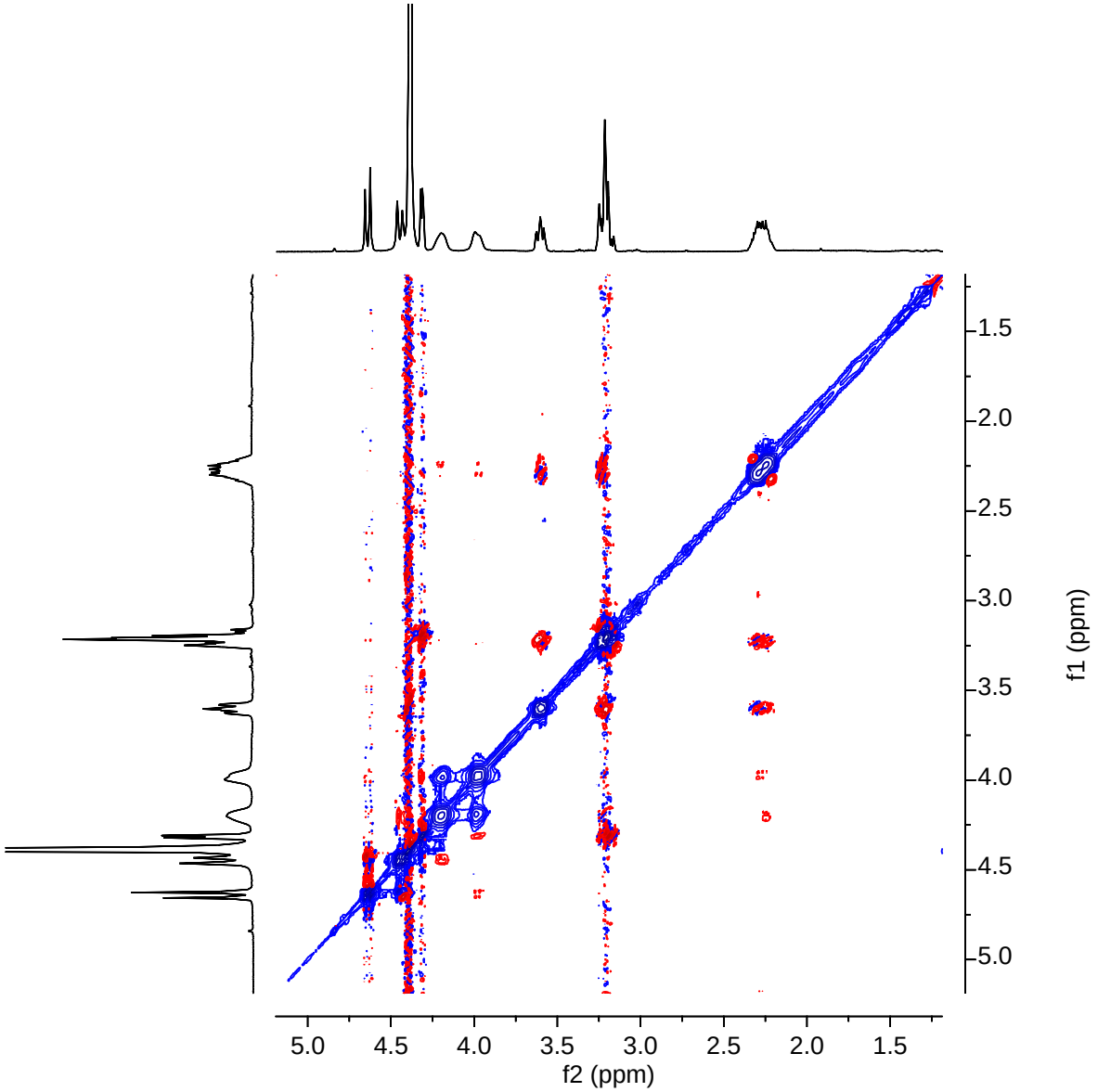

Figure S19. NOESY (500 MHz, D_2O, 335 K) of **2**.

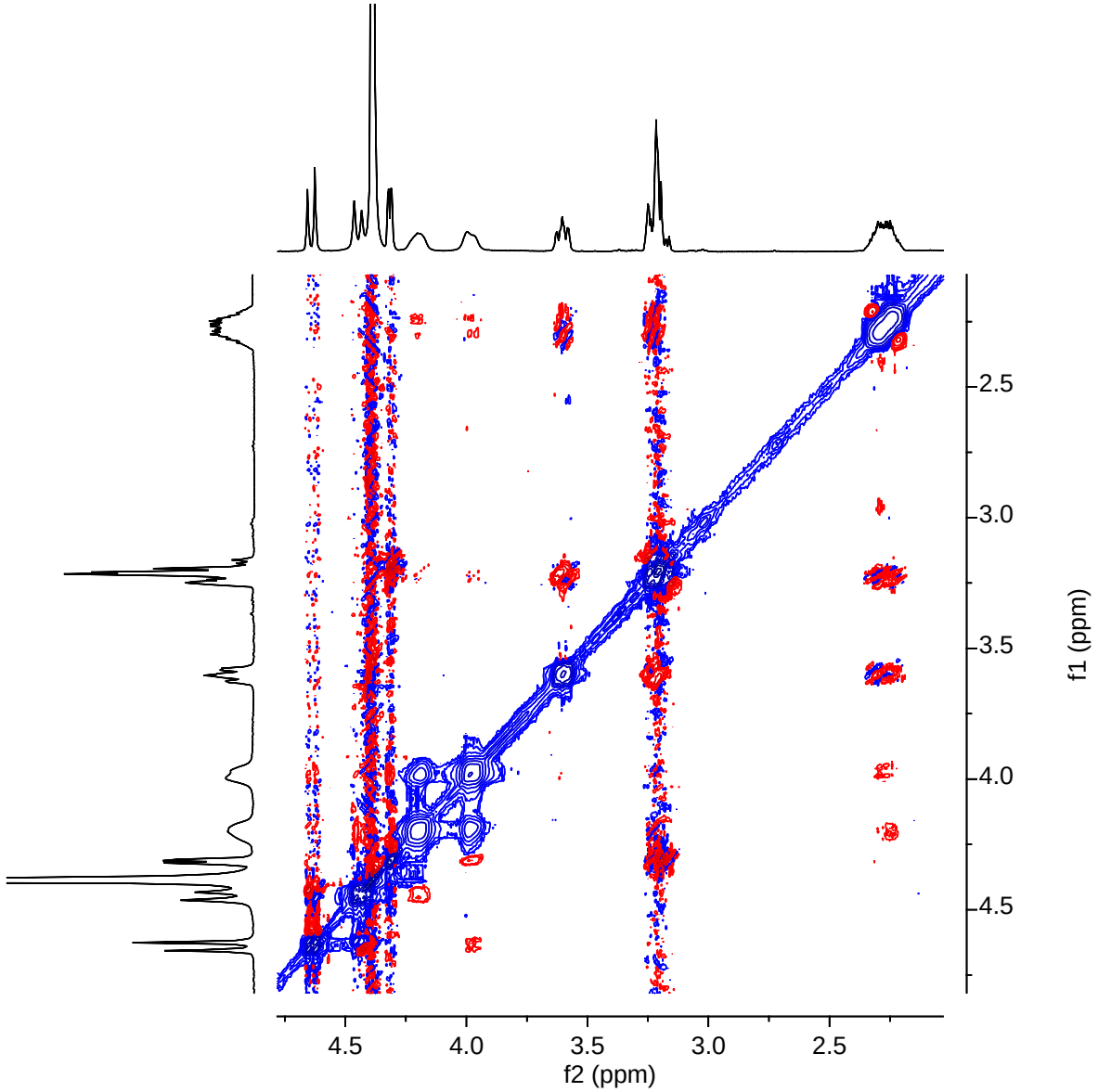

Figure S20. NOESY (500 MHz, D_2O, 335 K, range 2.10 – 4.75 ppm) of **2**.

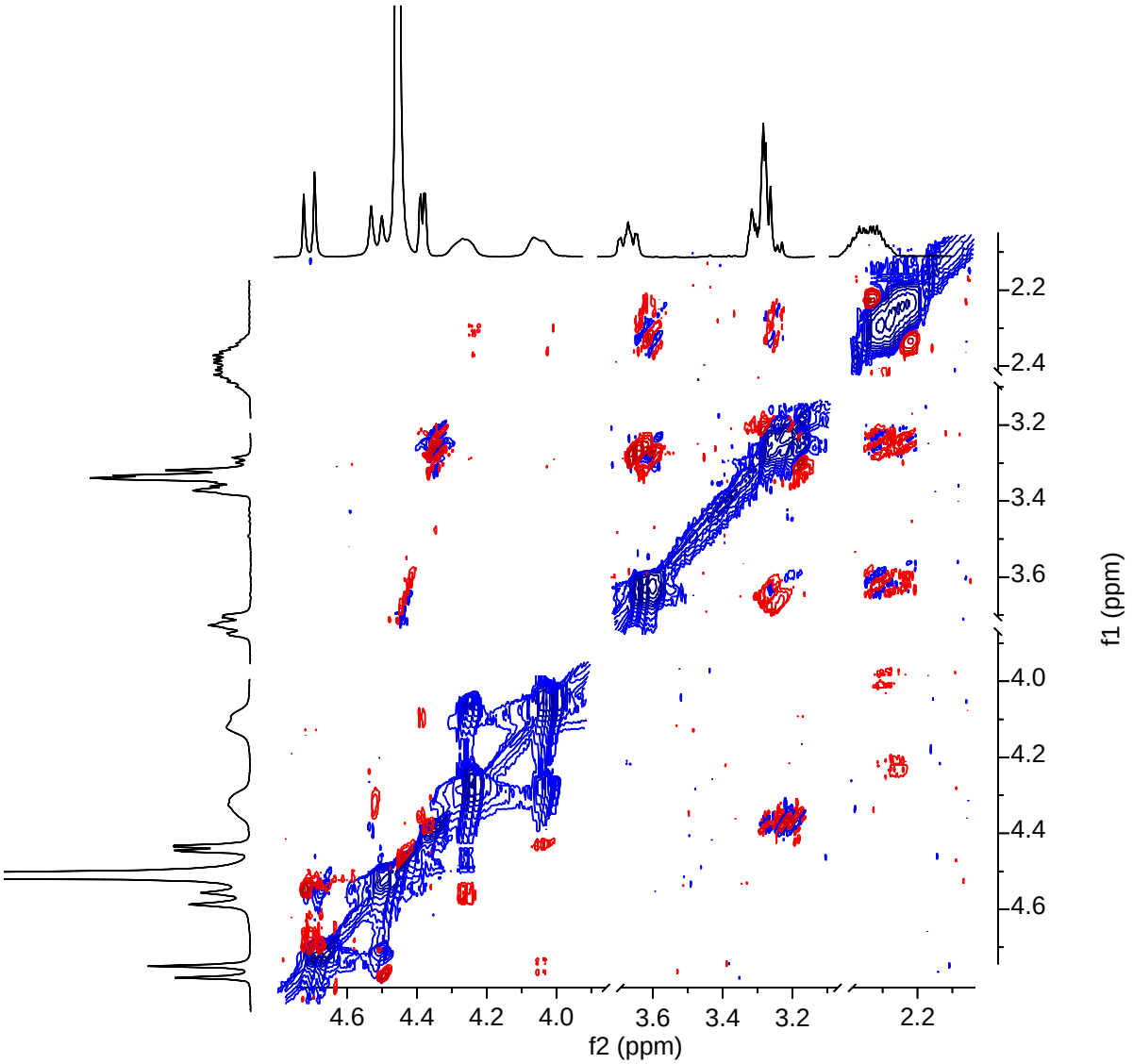

Figure S21. NOESY (500 MHz, D_2O, 335 K, range 2.10 – 4.75 ppm) of **2**. Signal-free areas are removed and t1 noise is reduced.

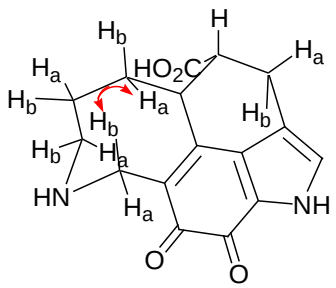

Figure S22. Predominant conformation of mycenarubin C (**2**) according to key NOE correlations (↔) and coupling constants in the ^1H NMR at 335 K in D_2O.

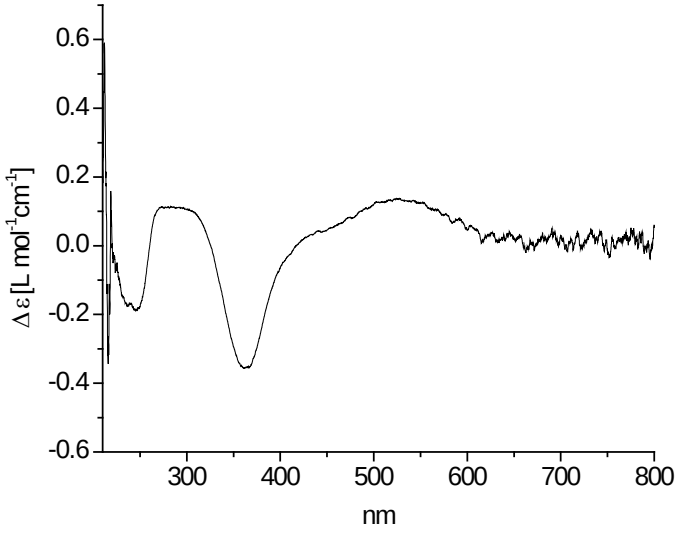

Figure S23. CD spectrum of mycenarubin C (**2**) recorded in H_2O.

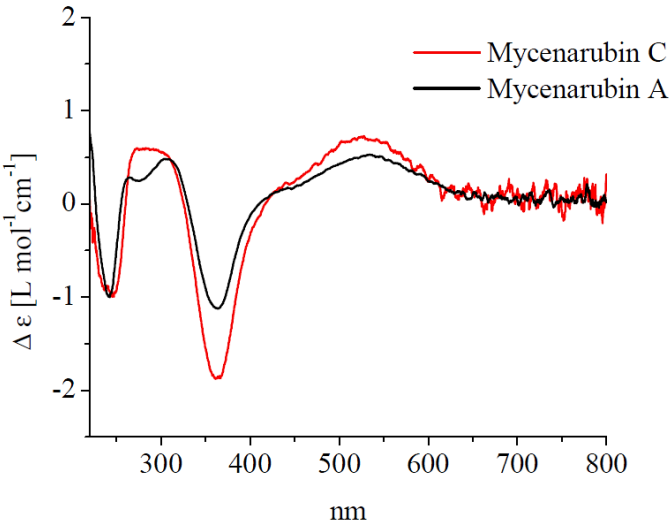

Figure S24. CD spectra of mycenarubin C (**2**) and mycenarubin A (**1**) recorded in H_2O.

Bioactivity tests with mycenarubin C (2)

Antimicrobal tests, method A

For plate diffusion assays, 0.15 mg (0.5 µmol) of mycenarubin C (**2**) were dissolved in 10 µL distilled and sterilised water, and dropped on paper discs (Ø 6 mm, thickness 0.5 mm). The paper discs were then dried under sterile conditions before being placed on agar plates inoculated with the respective test organism (*Azoarcus tolulyticus*, *Azospirillum brasilense*, *Azovibrio restrictus*, *Bacillus fastidiosus*, *Bacillus subtilis, Escherichia coli, Nocardioides simplex, Paenibacillus polymyxa, Sporosarcina pasteurii*, *Staphylococcus capitis, Mucor hiemalis*, and *Spinellus fusiger*). The plates were incubated at 37 °C for 24 h for *E. coli* and *B. subtilis*. The other bacterial cultures were incubated for 24 h at 30 °C. *M. hiemalis* was incubated at 25 °C for 24 h and *S. fusiger* at 12 °C for 11 days. For comparison with a positive control, the organisms were tested under the same conditions using 10 µL of an aqueous solution (1 mg/mL) of the antibiotic gentamycin (see Tables S1 and S2).

Antimicrobal tests, method B

A stock solution of mycenarubin C (**2**, 1 mg/mL in H_2O) was used for tests in 96-well microtiter plates. The tests were both performed with 2 µL and 20 µL of the stock solution, corresponding to 0.0066 and 0.066 µmol of **2** per well, respectively. As test organisms *Schizosaccharomyces pombe, Pichia anomala, Mucor hiemalis*, *Rhodotorula glutinis, Micrococcus luteus, Bacilus subtilis, Escherichia coli, Mycolicibacterium smegmatis, Chromobacterium violaceum,* and *Pseudomonas aeruginosa* were used. The tests were performed as described in Surup et al. 2013 (see Tables S1 and S2).[S8]

Tests for cytotoxicity of 2

Mycenarubin C (**2**) was also tested against the tumour cell lines L929 and KB3.1 as described in the literature[S9] but showed no activity.

Tests for biofilm inhibition

Mycenarubin C (**2**) was tested for biofilm inhibition against *Candida albicans* and *Staphylococcus aureus* in the same concentration as before as described in the literature[S10, S11] but failed to exhibit significant activities.

Test against the nematode *Caenorhabdis elegans*

Mycenarubin C (**2**) was tested against *Caenorhabditis elegans* nematodes (wild type strain, nematode suspension with approximately 500 nematodes/mL in M9 buffer) for nematicidal activity in 24-well microtiter plates (1 mL/well) as described in Rupcic et al. 2018[S12] but showed no activity up to 100 µg/ml after incubation at 20°C in the dark for 18 hours. For comparison a negative control (methanol) and a positive control (ivermectin) were used.[S12]

Table S1. Bioactivity tests of mycenarubin C (**2**) against selected bacteria.

Organism	**Gram**	**DSM-Nr.**	0.5 µmol **2** [a] 0.066 µmol **2** [b]	**Control** (1 mg/mL)
Azospirillum brasilense sp7 [a]	(-)	sp7*	n.i.	Gentamycin
Azovibrio restrictus [a]	(-)	23866*	n.i.	Gentamycin
Azoarcus totulyticus [a]	(-)	Td-1*	n.i.	Gentamycin
Bacillus fastidiosus [a]	(+)	73	n.i.	Gentamycin
Bacillus subtilis [a]	(+)	10	n.i.	Gentamycin
Chromobacterium violaceum [b]	(-)	30191	n.i.	Oxytetracyclin
Escherichia coli [a/b]	(-)	1116	n.i.	Gentamycin[a] Oxytetracyclin[b]
Micrococcus luteus [b]	(+)	1790	n.i.	Oxytetracyclin
Mycolicibacterium smegmatis [b]	(+)	ATTC 700084	n.i.	Kanamycin
Nocardioides simplex [a]	(+)	20130	n.i.	Gentamycin
Paenibacillus polymyxa [a]	(+)	36	n.i.	Gentamycin
Pseudomonas aeroginosa PA14 [b]	(-)	19882	n.i.	Gentamycin
Sporosarcina pasteurii [a]	(+)	33	n.i.	Gentamycin
Staphylococcus aureus [b]	(+)	346	n.i.	Oxytetracyclin
Staphylococcus capitis [a]	(+)	6717	n.i.	Gentamycin

[a] tested according to method A; [b] tested according to method B; n.i.: no inhibition; if not directly stated (e.g. ATCC, American Type Culture Collection) the cultures were obtained from DSMZ (Deutsche Sammlung von Mikroorganismen und Zellkulturen, Germany) with the corresponding DSM number. * provided by Prof. Dr. Reinhold-Hurek, University of Bremen.[S6]

Table S2. Bioactivity tests of mycenarubin C (**2**) against selected fungi.

Organism	**DSM-Nr.**	0.5 µmol **2** [a] 0.066 µmol of **2** [b]	**Control** 1 mg/mL Nystatin (20 µL)
Candida albicans [b]	1665	n.i.	i
Mucor hiemalis [a/b]	2656	n.i.	i
Rhodotorula glutinis [b]	10134	n.i.	i
Pichia anomala [b]	6766	n.i.	i
Schizosaccharomyces pombe [b]	70572	n.i.	i
Spinellus fusiger [a]	CBS 633.80	n.i.	/

[a] tested according to method A; [b] tested according to method B; n.i.: no inhibition; /: not tested; i: inhibition; if not directly stated (e.g. CBS, Centraalbureau voor Schimmelkultures, Netherlands) the cultures were obtained from DSMZ (Deutsche Sammlung von Mikroorganismen und Zellkulturen, Germany) with the corresponding DSM number.

Total synthesis of mycenarubin C (2)

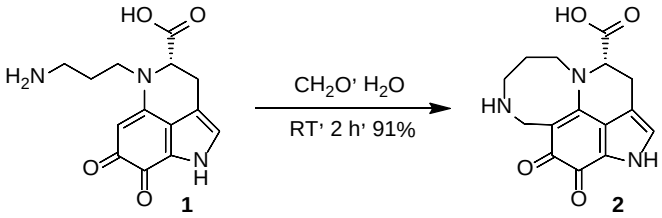

Scheme S1. Total synthesis of mycenarubin C (**2**) from **1**.

For the total synthesis of mycenarubin C (**2**) first mycenarubin A (**1**) was synthesised.[S2] Enantiopure mycenarubin A (**1**) (2 mg, 6.9 µmol) was dissolved in H_2O (1 mL), treated with an excess of formaldehyde (37 % aqueous solution, 5 µL, 69 µmol) and stirred at room temperature for two hours. The solvent was evaporated in vacuum. The crude reaction product was purified on a Sephadex LH-20 column with H_2O as eluent yielding mycenarubin C (**2**) (1.9 mg, 6.3 µmol) in nearly quantitative yield (91 %). The CD spectra (Figure S24) and the NMR spectra (Table S3) of mycenarubin C (**2**) isolated from *M. rosea* and of synthetic mycenarubin C agree very well with each other, thus confirming the proposed structure for **2**.

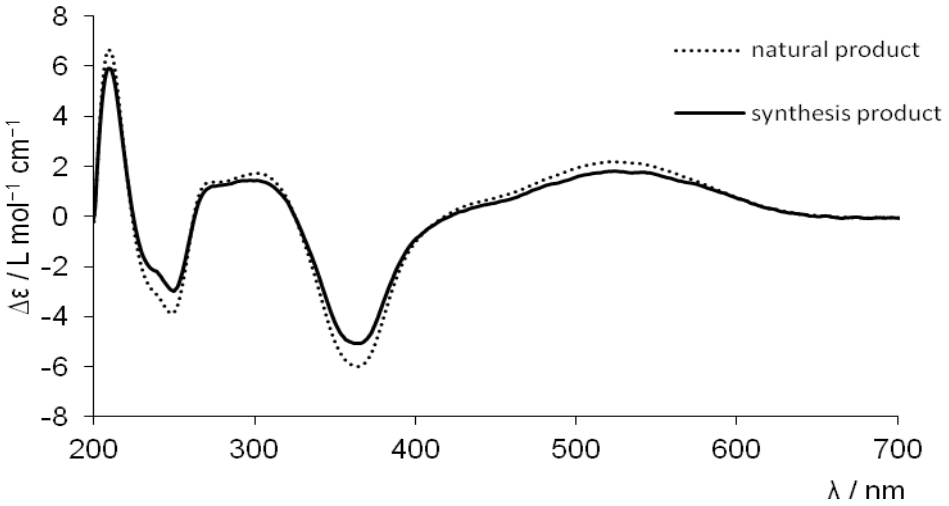

Figure S25. CD spectra of **2** isolated from *M. rosea* and of synthetic **2** in H_2O.

Table S3. NMR data of **2** isolated from *M. rosea* and of synthetic **2**.

#	Mycenarubin C (**2**) isolated from *M. rosea*		Synthetic mycenarubin C (**2**)	
	δ_C / ppm[a]	δ_H / ppm[b] (mult. *J* [Hz])	δ_C / ppm[c]	δ_H / ppm[d] (mult. *J* [Hz])
2	128.7 CH	7.13 (s)	128.6 CH	7.11 (s)
2a	119.6 C_q	-	119.6 C_q	-
3	26.2 CH_2	3.233 (dd, 16.7, 1.9, H_a)	26.2 CH_2	3.20 (m)
		3.18 (dd, 16.7, 6.3, H_b)		
4	72.8 CH	4.32 (dd 6.3, 1.9)	72.8 CH	4.30 (m)
5a	159.4 C_q	-	159.3 C_q	-
6	97.7 C_q	-	97.7 C_q	-
7	181.9 C_q	-	181.9 C_q	-
8	171.4 C_q	-	171.4 C_q	-
8a	126.4 C_q	-	126.4 C_q	-
8b	127.8 C_q	-	127.8 C_q	-
9	178.7 C_q	-	178.6 C_q	-
10	54.0 CH_2	4.20 (ddm, 14.7, 6.6, H_a)	53.9 CH_2	4.16 (m)
		3.98 (dm, 14.7, H_b)		3.98 (m)
11	27.4 CH_2	2.28 (dddd, 15.4, 6.6, 5.9, 3.7, 3.3, H_a)	27.4 CH_2	2.29 (m)
		2.24 (dddd, 15.4, 9.8, 4.2, 4.2, 3.3, H_b)		2.19 (m)
12	41.1 CH_2	3.60 (ddd, 13.1, 9.8, 3.7, H_a)	41.2 CH_2	3.56 (m)
		3.234 (ddd, 13.1, 5.9, 3.9, H_b)		3.20 (m)
14	42.5 CH_2	4.64 (d, 15.3, H_a)	42.5 CH_2	4.62 (d, 15.3, H_a)
		4.45 (d, 15.3 H_b)		4.46 (d, 15.3, H_b)

[a] Measured at 500 MHz at 335 K in D_2O. [b] Measured at 151 MHz at 330 K in D_2O. [c] Measured at 600 MHz at 330 K in D_2O. [d] Measured at 151 MHz at 330 K in D_2O.

Quantification of free formaldehyde in fruiting bodies of *Mycena* species

Calibration Data

Calibration curves obtained after GC-MS analysis with 1,2-dibromopropane (**6**) as internal standard, *O*-(2,3,4,5,6-pentafluorobenzyl)hydroxylamine (**5**) as derivatisation reagent and 2,4,5-trifluoro-acetophenone as surrogate to monitor the derivatisation.[S3]

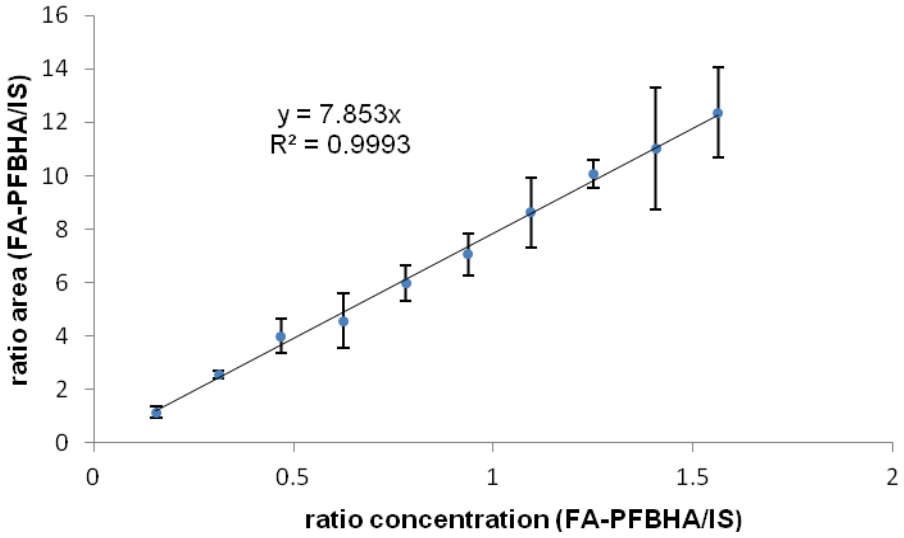

Figure S26. Calibration curve 1 (Range: 25 to 250 µg/L).

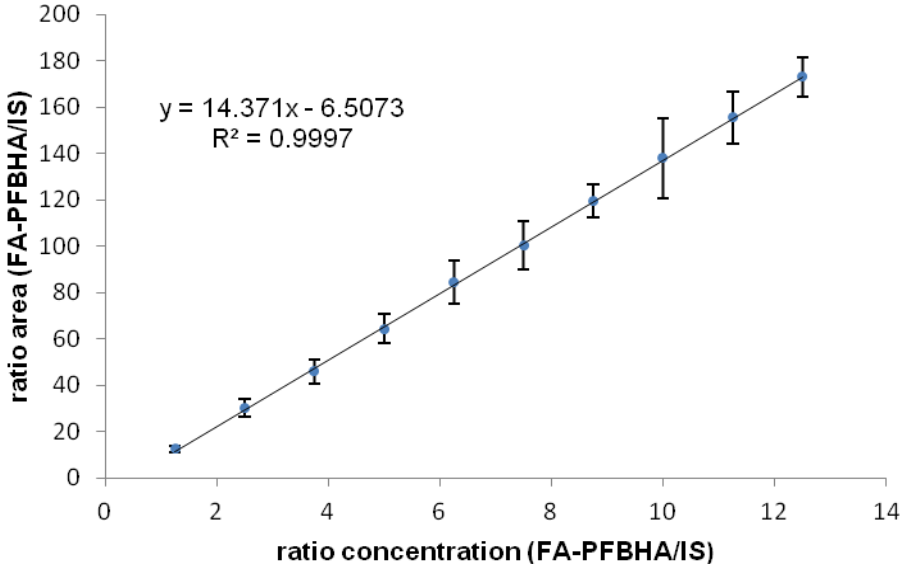

Figure S27. Calibration curve 2 (Range: 200 to 2000 µg/L).

The GC-MS measurements were performed using a Thermo Finnigan Trace DSQ with an EI-MS and an AS300 Autosampler (Thermo Finnigan, Thermo Fisher Scientific Inc., USA). Helium was used as carrier gas with a constant flow of 1 mL/min. Temperature program: Isotherm at 50°C for 1 min, then from 50°C with a linear gradient (4°C/min) to 220°C, after that with a second linear gradient (20°/min) to 250°C, then isotherm for 10 min at 250°C. For the separations an Optima® 5 ms Accent GC column

(Macherey-Nagel, 15 m x 0.25 mm ID, 0.25 µm film thickness) was used. Fur injection a PTV injector heated to 200°C was used in splitless-injection mode. The EI-mass spectrometer was operated either in positive full scan mode (mass range 34-600 u, 1.9763 scans/s, 1171.1 amu/s) or in the selected ion monitoring mode (SIM masses 121,123,181, scan time 0.36 s).

Equations to obtain calibration curve 1 and calibration curve 2

All calculations were performed as described in the literature[S4-6] according to the German norm of calibration (DIN 38 402 51A).[S4] For sample preparation, concentration factors had to be calculated in order to get the true amount of formaldehyde present in the samples. A dilution factor (f_d) for the spiking solutions and an enrichment factor (f_e) for the liquid-liquid extraction with *n*-hexane (see equation 1).

$$x_i = \frac{c_{Spiking-Solution} \cdot f_d}{f_e \cdot c_{IS}} = \frac{c(FA)\frac{mg}{L} \cdot 0.0001}{0.20 \cdot 800\,\mu\frac{g}{L}} \quad (1)$$

Furthermore, the concentrations were standardised to the concentration of the internal standard (c_{IS}).

Calibration curve 1

The calibration range was 25 to 250 µg/L in equidistant steps of 25 µg/L.

The residual standard deviation (equation 2) of the first calibration (s_{y1}) was calculated to be

$$s_{y1} = \sqrt{\frac{\Sigma(y_i - (a + bx_i))^2}{N-2}} = 0.228457 \quad (2)$$

For the first calibration, the standard deviation of variation (s_{xo}) is according to equation 3:

$$s_{xo} = \frac{s_{y1}}{b} = 0.0290929\mathbf{22} \quad (3)$$

This leads to a coefficient of variation (CV) as shown in equation 4:

$$CV = \frac{s_{xo}}{\bar{x}} \cdot 100\% = 3.38\% \quad (4)$$

Mandel's fitting test was applied by comparison of the residual standard deviations of a linear regression (s_{y1}), polynomic regression 2nd grade (s_{y2}) and a subsequent conducted difference (DS^2) according to equation 5:

$$DS^2 = (N-2) \cdot s_{y1} - (N-3) \cdot s_{y2} \quad (5)$$

N = number of calibration points. These values were used to generate a test value (equation 6),

$$F_{calc} = \frac{DS^2}{s_{y2}^2} = 0.5927009\mathbf{2} \quad (6)$$

This test value was compared to a tabular f-value ($F_{tab\ (\alpha = 0.01;\ 1,\ n-3)}$ = 8.40). The test value was smaller than the tabular value; therefore, the regression was proven to be linear.

The minimum detection level (MDL) was estimated to be $3.052 \cdot 10^{-8}$ mol/L by the following equation 7[S4]:

$$MDL = S \cdot t_{(n-1,\,1-alpha=0.99)} \quad (7)$$

With: S = standard deviation of replicate analysis, n = number of replicates, n - 1 = degrees of freedom and $t_{(n-1,\,1-alpha=0.99)}$ = student`s t value for the 99% confidence level. The concentration estimated to be near the MDL, 2 to 3 times the noise level, was 5 µg/L. The number of replicates was 7.

The limit of detection (LOD) and the limit of quantification (LOQ) were determined using the following equations 8 to 11:[S5]

$$y_{LOD1} = b_1 + s_{y1} \cdot t_{(f=8,\,P=0.95)} \sqrt{\frac{1}{N_c} + \frac{1}{N_a} + \frac{\bar{x}^2}{\sum_i^N (x_i - \bar{x})^2}} \quad (8)$$

$$x_{LOD1} = \frac{y_{LOD1} + a_1}{b_1} \quad (9)$$

$$LOD_1 = \frac{x_{LOD1} \cdot 0.0008 \frac{g}{L}}{30 \frac{g}{mol}} \quad (10)$$

$$LOQ_1 = 2 \cdot LOD_1 \quad (11)$$

Therefore, the values of LOD_1 and LOQ_1 were taken as $2.2 \cdot 10^{-7}$ and $4.4 \cdot 10^{-7}$ mol/L.

Experiments in regard to the recovery of the regression model showed an average of 91.5 ± 5.6% (n = 6), by adding formaldehyde spiking solutions (75 mg/L) to half of the samples already containing (50 mg/L) formaldehyde.

Calibration curve 2

For stored fruiting bodies, the concentration range was found to be significantly higher. Therefore, a calibration range of 200 to 2000 µg/L in equidistant steps of 200 µg/L was used. The second regression model obtained was: y = 14.371 (± 0.093) x – 6.5073, $r^2 = 0.9997$. The residual standard deviation (s_{y1}) was calculated to be s_{y1} = 0.9534109. For the second calibration, the standard deviation of variation (s_{xo}) was s_{xo} = 0.06790676 which leads to a coefficient of variation (CV) at CV = 0.99%. The area under the curve and the concentrations were standardised on the values of the internal standard 1,2-dibrompropane. Mandel's fitting test was applied for the mathematical verification of linearity resulting in (F_{calc} = 0.795 *vs*. $F_{tab\ (\alpha = 0.01;\ 1,\ n-3)}$ = 8.40), proving a linearity of the regression. LOD_2 and LOQ_2 were calculated as in calibration 1 to be $3.5 \cdot 10^{-6}$ and $7.07 \cdot 10^{-6}$ mol/L.

Results

Both calibration curves fit the criteria of linear regression and can be used to measure the formaldehyde content in fruiting bodies. The measured values were given with their respective confidence interval (CI) which was calculated as shown in the following equations 12 and 13:[S6]

$$\hat{\bar{x}}_{1,2} = \frac{\hat{\bar{y}} - a}{b} \pm CI(\hat{\bar{x}}) \quad (12)$$

$$\hat{\bar{x}}_{1,2} = \frac{\hat{\bar{y}} - a}{b} \pm s_{xo} \cdot t_{(N-2;\,0.95)} \cdot \sqrt{\frac{1}{N} + \frac{1}{\hat{n}} + \frac{(\hat{\bar{y}} - \bar{y})^2}{b^2 * \sum_{i=1}^{N}(x_i - \bar{x})^2}} \quad (13)$$

N = number of calibration pairs, $\hat{n}$ = number of replicate measurements, b = slope of the regression, $\hat{\bar{y}}$ = median of the probe concentration, $\bar{x}$ and $\bar{y}$ median of the calibration data.

A systematic proportional matrix effect was found in the differences of the slopes and included in the calculations as a correction factor. This leads to the concentration c, calculated according to the following equation 14:[S5]

$$c = \frac{\hat{\bar{x}} - 0.4785}{1.837} \quad (14)$$

Then, the formaldehyde concentration in µg/g fruiting body was determined using equation 15:

$$c(FA) = \frac{c \cdot 800\ {}^{\mu g}/_{L} \cdot 0.022L}{m(fruiting\ body)} \quad (15)$$

The calculations of the t-test values for the comparison of measured medians are shown in formula 16:

$$t' = \frac{|\bar{x}_1 - \bar{x}_2|}{\sqrt{\frac{n_1 + n_2}{n_1 \cdot n_2} \cdot \frac{(n_1 - 1) \cdot s_1^2 + (n_2 - 1) \cdot s_2^2}{n_1 + n_2 - 2}}} \quad (16)$$

These t-test vales were compared to the critical t-table values for the significance level of 0.005. If t-test value ≥ t-table value, then the difference in the medians is significant.

Selected chromatograms and spectra used for the quantification of formaldehyde

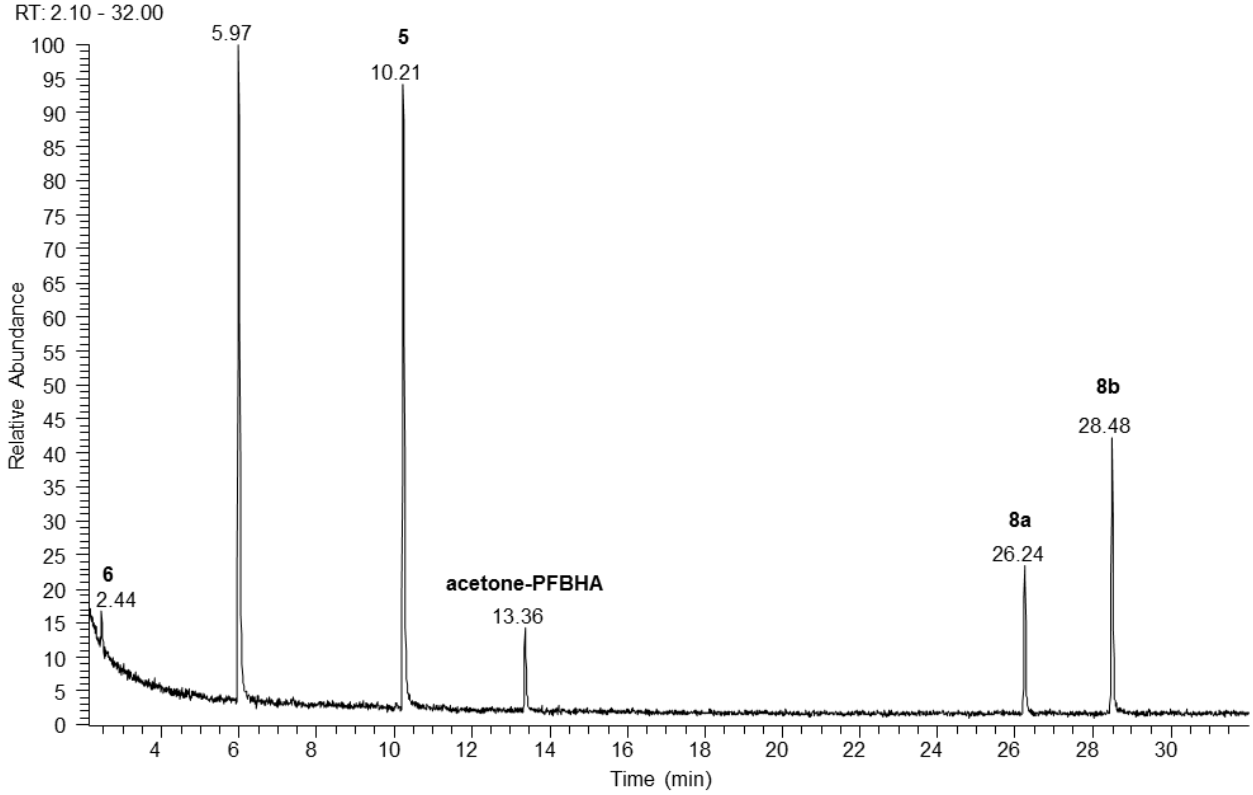

Figure S28. Selected GC-(+)-EI-MS full scan chromatogram of compounds **5** – **8** in a blank sample. **5** R_i = 1084.69, **6** R_i = 876.35, **7** R_i = 1012.00, **8a** R_i = 1561.03, and **8b** R_i = 1641.24.

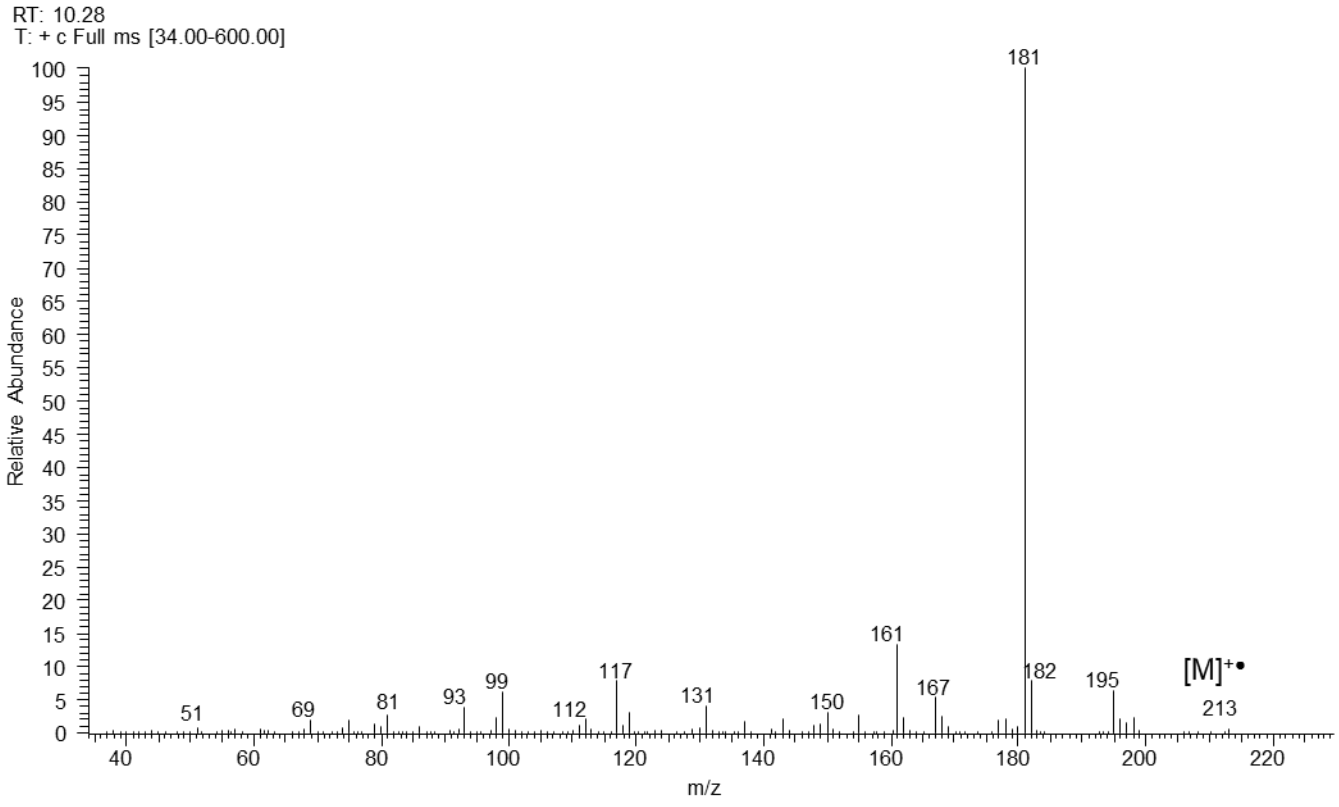

Figure S29. (+)-EI-MS spectrum of *O*-(2,3,4,5,6-pentafluorobenzyl)hydroxylamine (PFBHA, **5**).

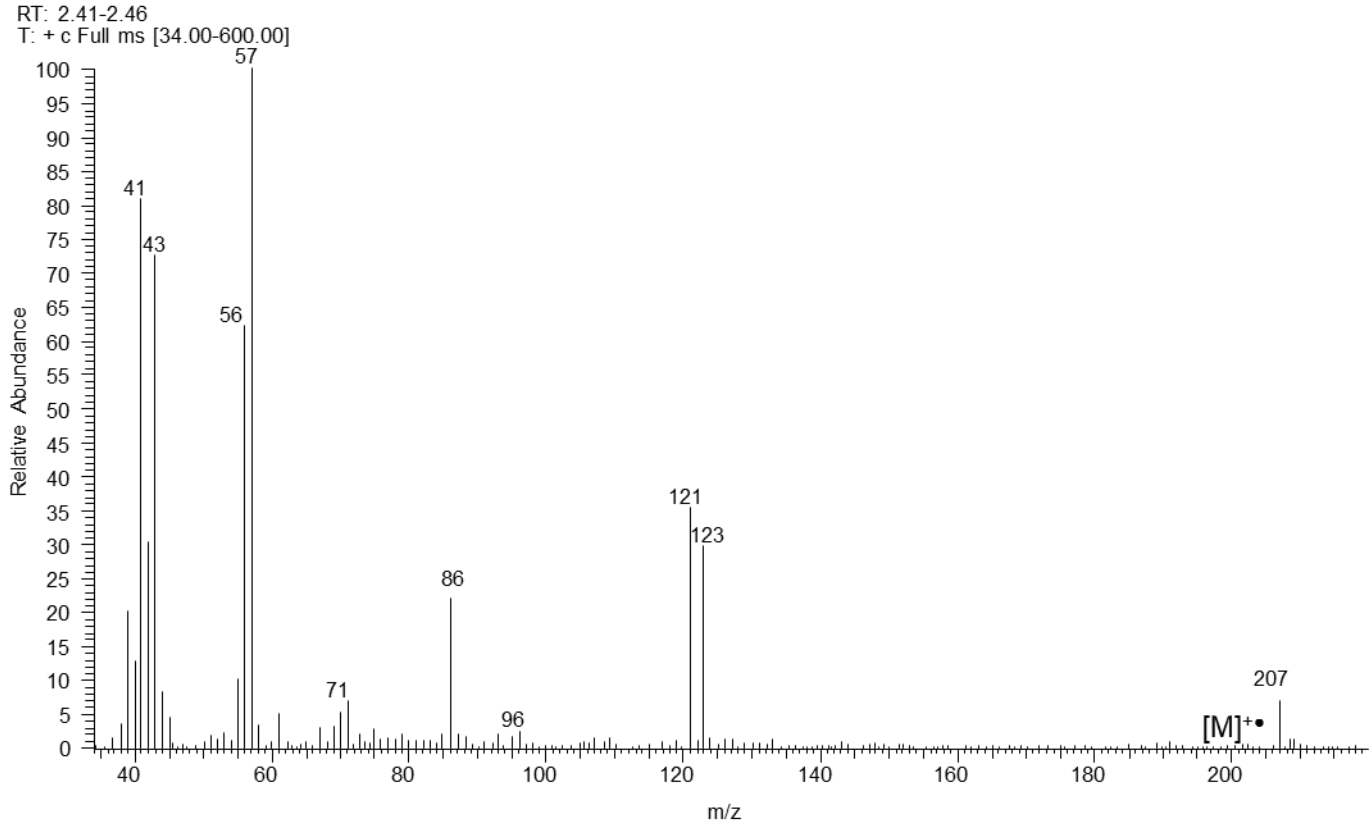

Figure S30. (+)-EI-MS spectrum of 1,2-dibromopropane (**6**).

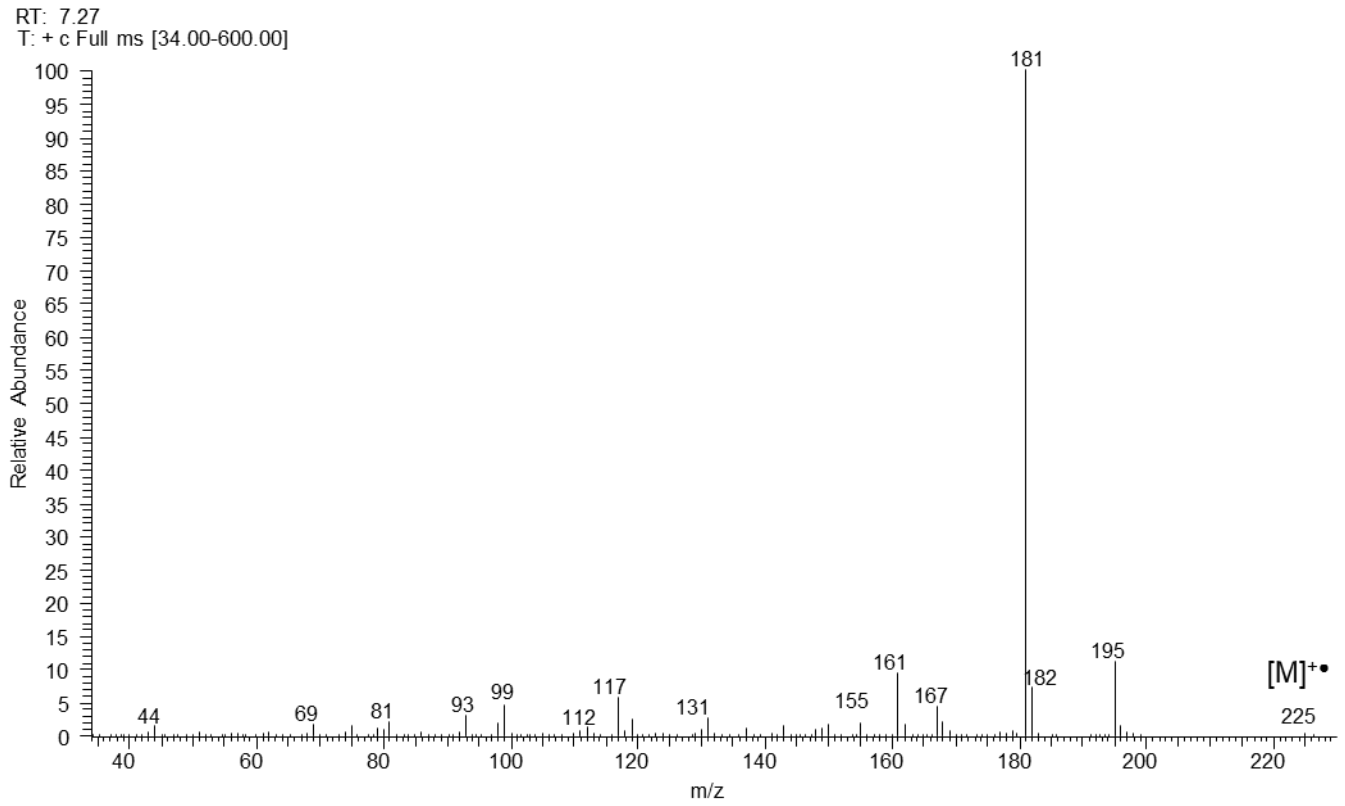

Figure S31. (+)-EI-MS spectrum of formaldehyde-*O*-((pentafluorophenyl)methyl)oxime (**7**).

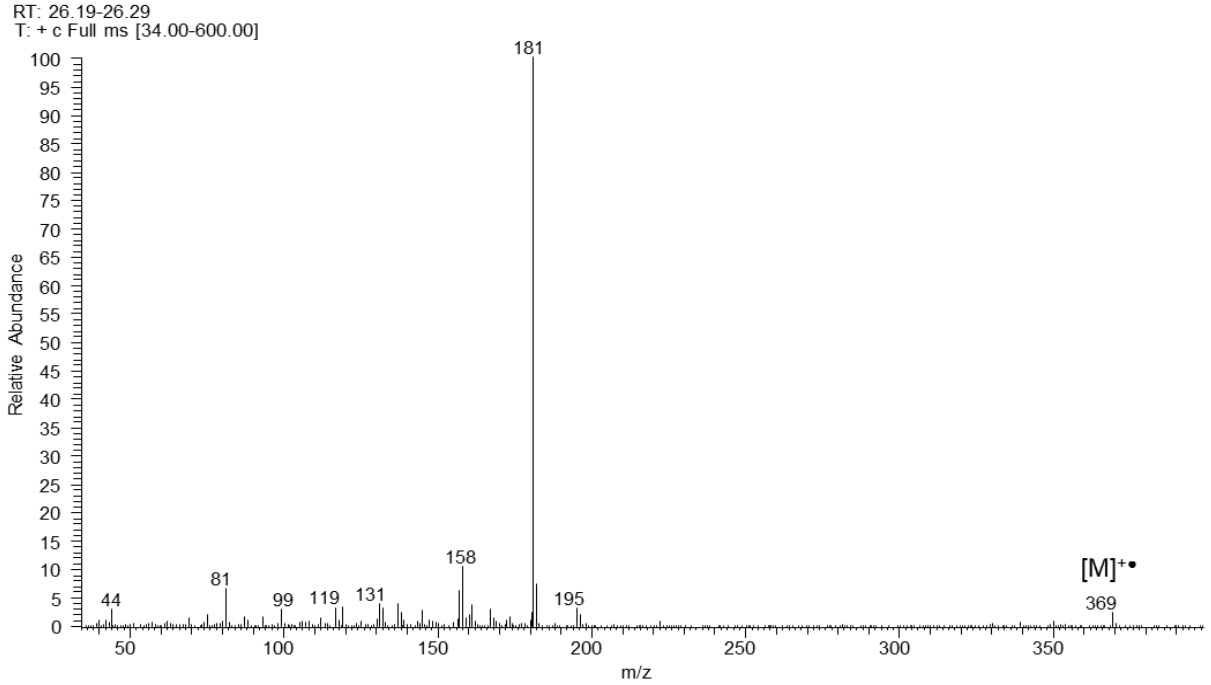

Figure S32. (+)-EI-MS spectrum of (*E*)-1-(2',4',5'-trifluorophenyl)ethanone-*O*-(pentafluorophenyl)-methyl)oxime (**8a**).

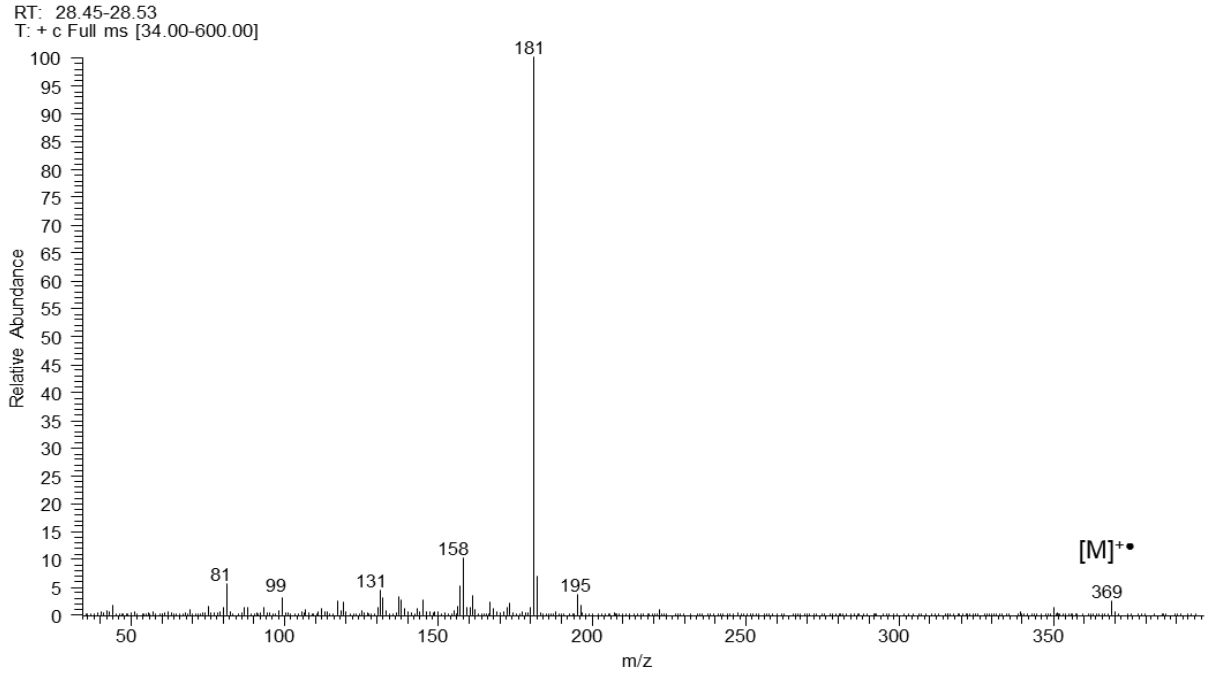

Figure S33. (+)-EI-MS spectrum of (*Z*)-1-(2',4',5'-trifluorophenyl)ethanone-*O*-(pentafluorophenyl)-methyl)oxime (**8b**).

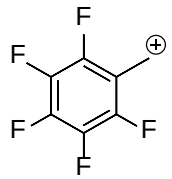

9

Figure S34. Basis ion *m/z* 181 of compounds **5** – **8** derivatised with **5**.

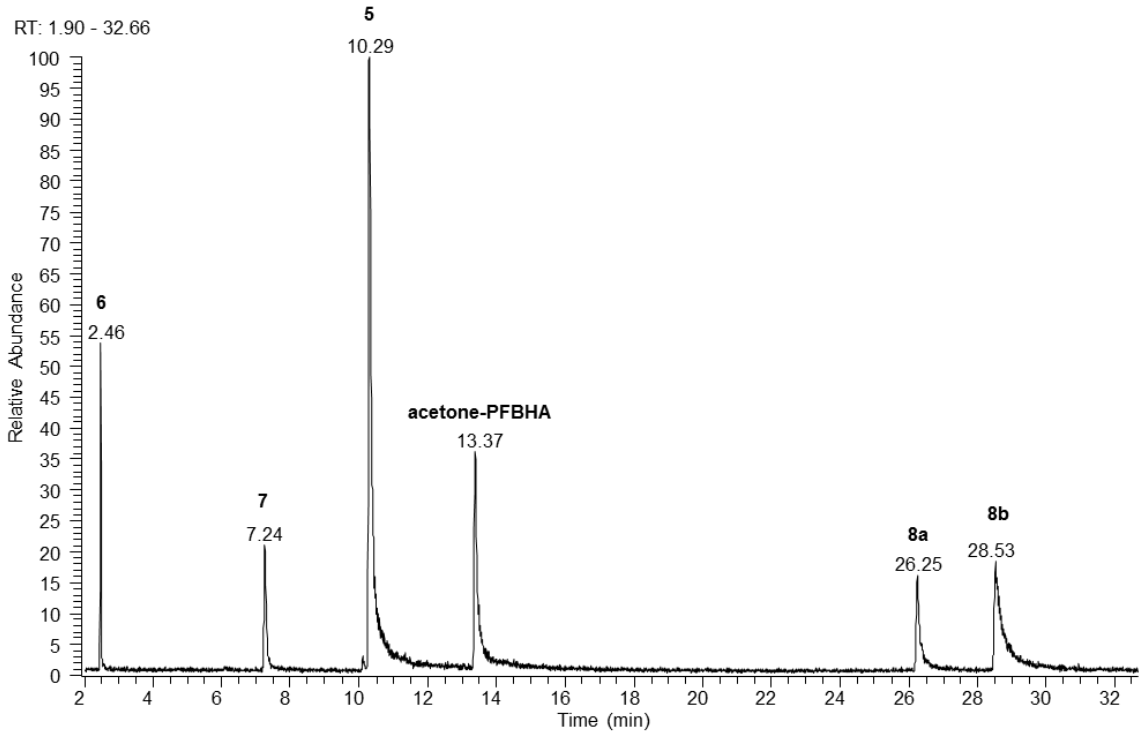

Figure S35. Selected ion monitoring chromatogram of compounds **5** – **8**.

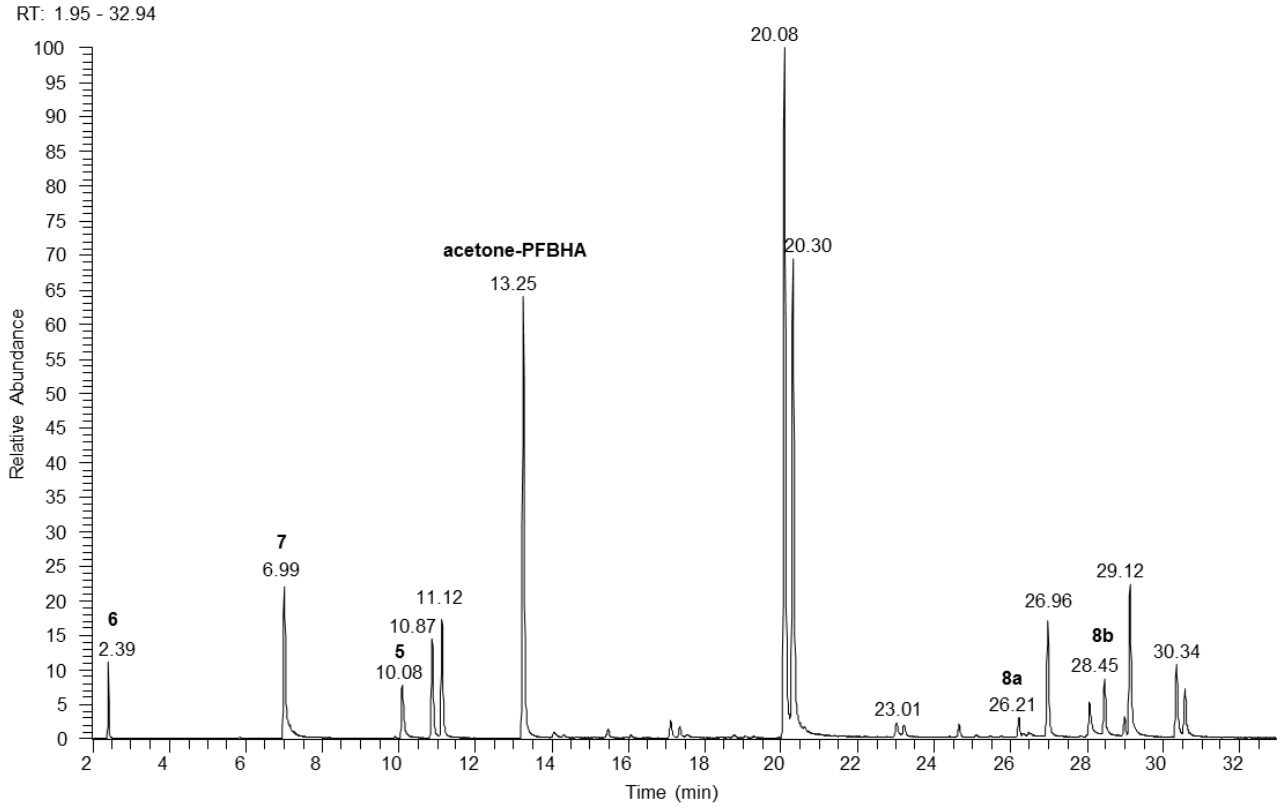

Figure S36. Selected ion monitoring chromatogram of compounds **5** − **8** in *M. rosea* matrix.

Results of the quantification of formaldehyde in fruiting bodies of *Mycena rosea*

Table S4. Influence of the location and age on the formaldehyde content of freshly collected fruiting bodies of *M. rosea*.

Collection	mean ± CI µg/g	number of replicas
Studentenwald Bayreuth (114/16) 14.10.2016 (5 days 4°C)	8.30 ± 0.80	n = 18
Pupplinger Au (115/16) 16.10.2016 (3 days 4°C) 4°C for 15 more days	2.79 ± 0.31 6.38 ± 0.33	n = 18 n = 12
Mühltal (116/16) 16.10.2016 (3 days 4°C)	5.04 ± 1.06	n = 18
Leutstetten (118/16) 16.10.2016 (3 days 4°C)	3.82 ± 0.82	n = 18
Breitbrunn (144/16) 21.10.2016 (5 days 4°C)	2.17 ± 0.19	n = 6
Mühltal (149/16) 22.10.2016 (4 days 4°C)	2.17 ± 0.37	n = 6
Mühltal (150/16) 22.10.2016 (4 days 4°C) - pale cap 2.36 / 4.68 g - young 1.49 / 1.39 g - medium age 3.77 / 3.86 g - old 1.57 / 2.33 g	3.28 ± 0.42 1.84 ± 0.24 3.45 ± 0.12 2.89 ± 0.22 2.46 ± 0.43	n = 36 n = 6 n = 6 n = 6 n = 6
Rieden (158/16) 22.10.2016 (4 days 4°C)	4.24 ± 0.67	n = 6
Breitbrunn (167/16) 23.10.2016 (3 days 4°C)	4.05 ± 0.33	n = 6
Mühltal (191/16) 29.10.2016 (4 days 4°C)	4.10 ± 0.39	n = 12
Leutstetten (196/16) 30.10.2016 (3 days 4°C)	5.44 ± 0.71	n = 12
Breitbrunn (224/16) 06.11.2016 (2 days 4°C)	4.72 ± 0.77	n = 12
Average of all freshly collected collections	**3.89 ± 0.50**	**n = 204**
(infested) Breitbrunn (168/16) 23.10.2016 (3 days 4°C)	3.63 ± 0.78	n = 6
(infested) Mühltal (215 /16) 06.11.2016 (2 days 4°C)	4.66 ± 0.69	n = 18
Average of all infested collections	**4.15 ± 0.74**	**n = 24**

The average formaldehyde concentration (5.44 ± 0.71 µg/g) of collection 196/16 was used in Figure 3 and in the text of the manuscript, because from the same collection also the average formaldehyde content after 72 days of storage at –32°C was determined (see Table S6). The average formaldehyde concentration of all collections of fresh fruiting bodies was 3.89 ± 0.50 µg/g.

Table S5. Influence of storage at −32°C on the amount of formaldehyde in fruiting bodies (fb) of *M. rosea*.

Collection of frozen fruiting bodies (Storage at −32°C)	**mean ± CI / µg/g**	**number of replicas**
196/16 (72 days) 6.56 g	30.4 ± 1.1	n = 18
196/16 (107 days) 6.04 g (3 fb) [a]	80.9 ± 1.3	n = 9
196/16 (121 days) 13.45 g (2 fb) [a]	170.2 ± 2.9	n = 18
215/16 (119 days, infested) 12.94 g (1.5 fb)	36.4 ± 1.0	n = 18
131/15 (506 days) 6.77 g (2.5 fb)	24.4 ± 1.7	n = 9
045/14 (882 days) 6.01 g (2.5 fb)	24.1 ± 1.5	n = 9

[a] These collections show much elevated concentrations of formaldehyde. These collections were opened several times for removing fungi. For that time (some minutes), they were kept at room temperature). Obviously, partial thawing of the fruiting bodies increases the formaldehyde concentration significantly.

Table S6. Formaldehyde content in fresh and in stored fruiting bodies of *M. rosea* and *M. pura*.

Species (stored at −32°C / days)	**mean ± CI / µg/g**	**number of replicas**
M. rosea (fresh) collection 196/16	5.4 ± 0.7	n = 18
M. pura (fresh), collection 217/16	2.0 ± 0.5	n = 18
M. rosea (72 days at –32°C), collection 196/16	30.4 ± 1.1	n = 18
M. pura (70 days at –32°C), collection 217/16	14.8 ± 1.3	n = 18

Feeding experiment with CD_3OD into fruiting bodies of *M. rosea*

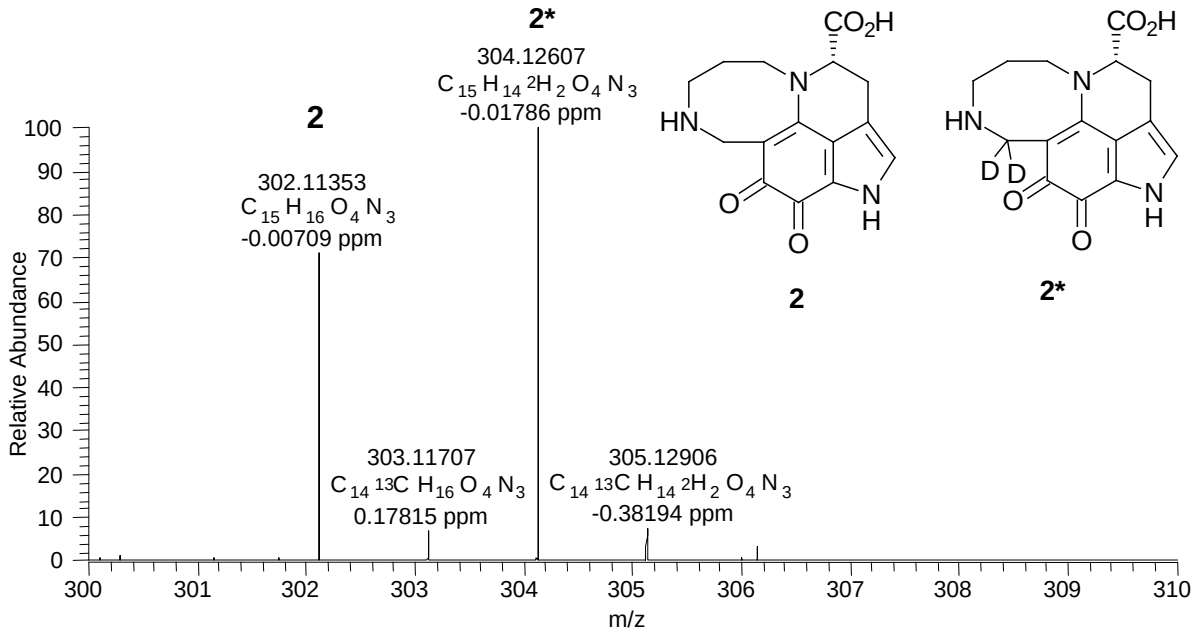

Figure S37. HR-(+)-ESI-MS showing the incorporation of two deuterium atoms in mycenarubin C isolated from fruiting bodies of *M. rosea* after feeding with CD_3OD. Mycenarubin C (**2**) represents the unlabelled species and **2*** the labelled species with two deuterium atoms originating from fed CD_3OD.

Determination of the relative ratio of the amount of 2 to the amounts of 1 and 2

To determine the relative ratio of the amount of mycenarubin C (**2**) to the amounts of mycenarubin A (**1**) and C (**2**) a fruiting body of *M. rosea* was extracted with H_2O-MeCN (50/50 v/v), pre-purified using an RP-18ec cartridge (H_2O then H_2O-MeCN (50/50 v/v) as eluent. The mycenarubins **1**, **2** and **3** were found in the H_2O-MeCN fraction. The compounds in this fraction were separated on an analytical Nucleodur RP-18ec column (250 mm × 3 mm, 100-5, Macherey-Nagel) using the following H_2O (+ 0.1% HOAc)/MeCN gradient: For 10 min 100% H_2O + 0.1% HOAc, then within 40 min linear to 100% MeCN, flow rate 0.660 mL/min). The measurements were carried out with an HPLC-UV/ESI-MS instrument (LCQ Thermo Finnigan, HPLC Hewlett Packard equipped with a PDA detector). For the calculation of the ratio of the amount of mycenarubin C (**2**) to the summarised amounts of mycenarubin A (**1**) and C (**2**), the peak areas of mycenarubin A (**1**) and mycenarubin C (**2**) were measured at λ = 360 nm using the software Xcalibur 2.0 (Thermo).

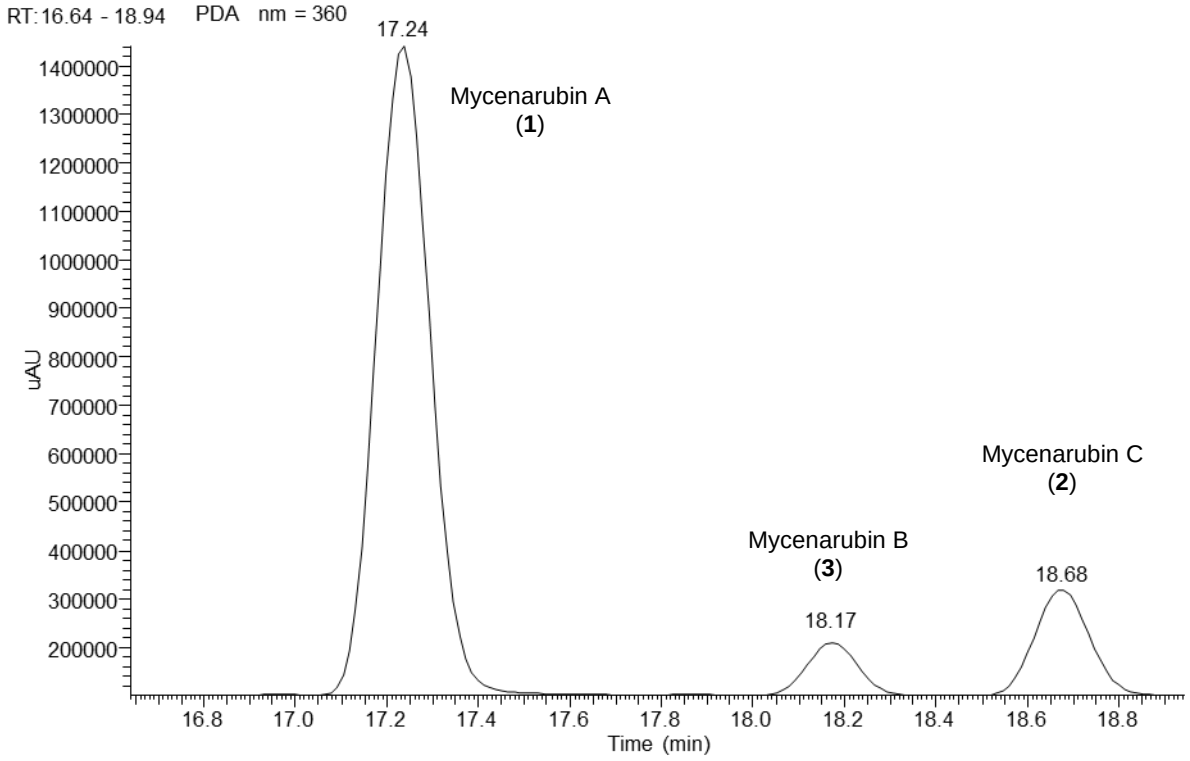

Figure S38. Analytical HPLC-UV chromatogram (λ = 360 nm) of a crude extract of *M. ro*sea.

Table S7. Influence of storage time on the relative amount of mycenarubin C (**2**) in relation to the summarised amounts of **1** and **2**) in fruiting bodies of *M. rosea*. The relative amounts of **1** and **2** were detemined by measurement of the the peak areas of **1** and **2** at λ = 360 nm in the HPLC-UV.

Collection number of fruiting bodies stored at −32°C	**Mean ± std / %**	**Number of replicas**
117/16 (dry weight, 209 days) 12.92 g	11.1 ± 3.0	n = 12
117/16 (wet weight, 209 days) 12.12 g	12.0 ± 0.3	n = 12
196/16 (107 days) 6.04 g (3 fb)	7.8 ± 0.2	n = 9
196/16 (121 days) 13.45 g (2 fb)	17.0 ± 1.0	n = 6
215/16 (119 days, infested) 12.94 g (1.5 fb)	3.0 ± 0.5	n = 6
131/15 (506 days) 6.77 g (2.5 fb)	1.9 ± 1.1	n = 3
045/14 (882 days) 6.01 g (2.5 fb)	1.7 ± 0.1	n = 3
050/10 (2323 days) 12.84 g	38.7 ± 0.6	n = 12
065/06 (3764 days) 12.85 g	95.5 ± 1.3	n = 12

Biological tests with formaldehyde against the mycoparasite *Spinellus fusiger*

Each amount of formaldehyde and the control H_2O was tested ten times. Spores of *S. fusiger* were applied on BPM media[S13] at 12 °C. After three days the first signs of growth (single hyphae) were visible on each plate. Then 10 µL of a differently concentrated formaldehyde solutions were applied onto paper discs and placed on the centre of the plates.

Table S8. Inhibition zones in dependence of the amount of formaldehyde applied on the paper disk nine days after application of formaldehyde to mycelial cultures of *S. fusiger*. The numbers represent the average diameters of the inhibition zones of ten plates used for each concentration. Measured were the minimal distances between paper disc and the mycelia.

	H_2O (Control)	**0.333 µmol CH_2O**	**0.665 µmol CH_2O**	**0.333 µmol CH_2O**	**0.4995 µmol CH_2O**	**0.6667 µmol CH_2O**	**0.8325 µmol CH_2O**	**1.665 µmol CH_2O**	**8.325 µmol CH_2O**
Inhibition zone [cm]	(5 of 10) n. i. 0.7 ± 0.8	(6 of 10) n. i. 0.7 ± 1.2	0.9 ± 0.4	1.5 ± 0.5	1.6 ± 0.4	1.6 ± 0.3	1.6 ± 0.3	3.4 ± 1.4	(9 of 10) n. g. 5.5

n. i.: no inhibition, paper disc overgrown with mycelial culture of *S. fusiger*; n. g.: no growth visible.

Identification of gallic acid in mycelial cultures of *S. fusiger*

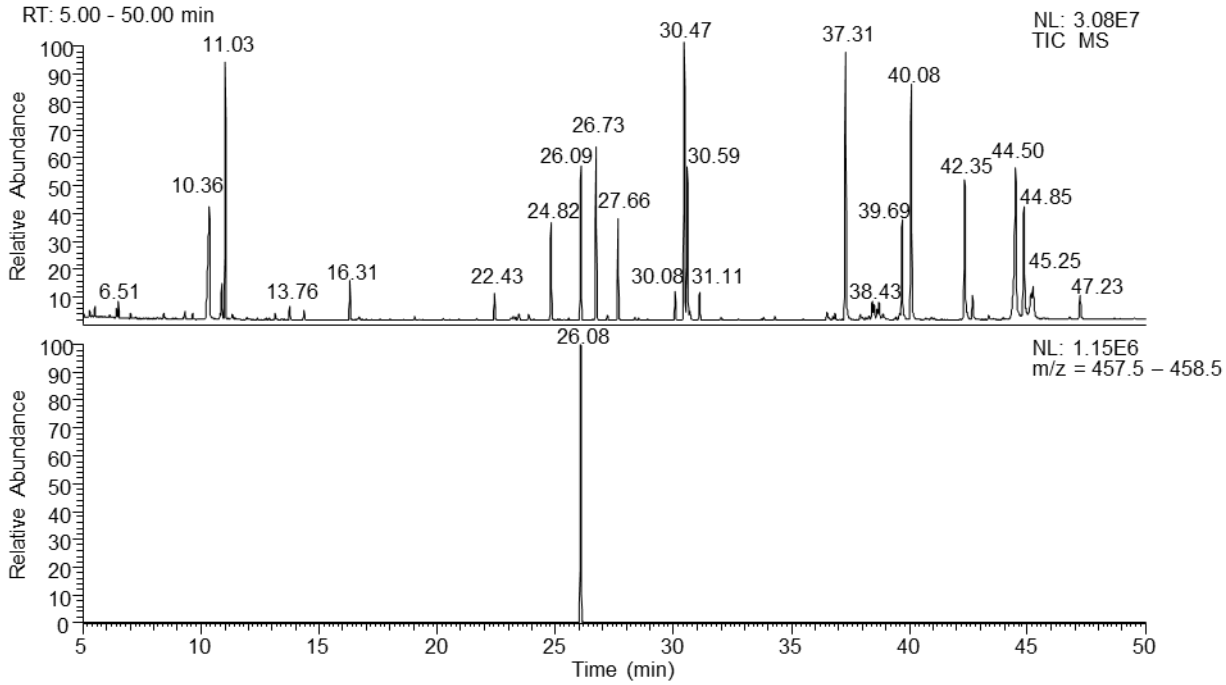

Figure S39. GC-EI-MS chromatograms of a pertrimetylsilylated methanol/ethyl acetate extract of three *S. fusiger* cultures (CBS 633.80, grown on BPM medium for 23 days at 12°C). The pertrimethylsilylation was done with MSTFA. Top: Total ion chromatogram. Bottom: Extracted ion chromatogram representing the molecular ion of pertrimetylsilylated gallic acid (R_i = 2007.65).

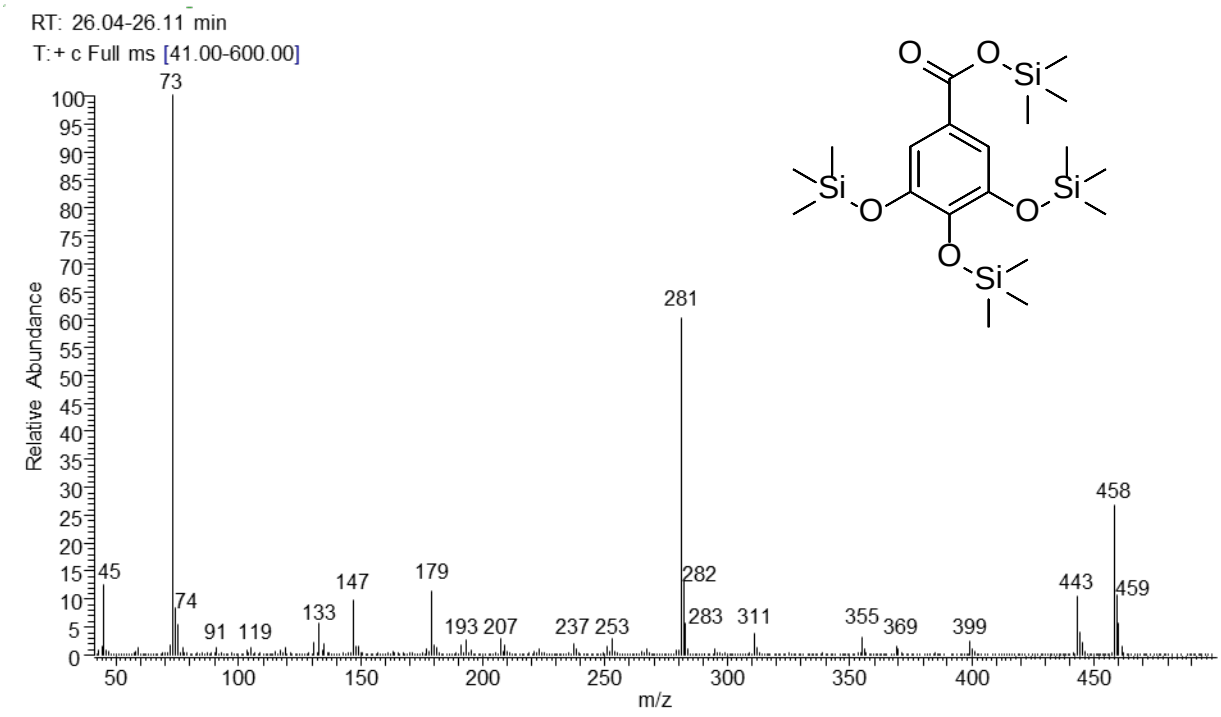

Figure S40. GC-(+)-EI-MS of gallic acid pertrimethylsilylated with MSTFA.

References

[S1] J. S. Lohmann, S. Wagner, M. von Nussbaum, A. Pulte, W. Steglich, P. Spiteller, *Chemistry* **2018**, *24*, 8609–8614.

[S2] J. Backenköhler, B. Reck, M. Plaumann, P. Spiteller, *Eur. J. Org. Chem.* ***2018*****,** 2806–2816.

[S3] J. W. Munch, D. J. Munch, S. D. Winslow, S. C. Wendelken, B. V. Pepich, *United States Environmental Protection Agency*, Ohio, **1998**, pp. 1–37.

[S4] German Norm for Calibration: DIN 38 402 51A

[S5] J. A. Glaser, D. L. Foerst, G. D. McKee, S. A. Quave, W. L. Budde, *Am. Chem. Soc*. **1981**, *15*, 1426–1435.

[S6] W. Funk, V. Dammann, G. Donnevert, *Qualitätssicherung in der Analytischen Chemie*. 2nd Ed., Wiley-VCH Verlag, **2005**, pp. 1–50.

[S7] B. Reinhold-Hurek, T. Hurek, *Int. J. Syst. Evol. Microbiol.* **2000**, *50*, 649–659.

[S8] F. Surup, K. I. Mohr, R. Jansen, M. Stadler, *Phytochemistry* **2013**, *95*, 252–258.

[S9] F. Surup, S. Halecker, M. Nimtz, S. Rodrigo, B. Schulz, M. Steinert, M. Stadler, *Steroids* **2018**, *135*, 92–97.

[S10] L. Z. S. Brambillaa, E. H. Endo, D. A. G. Cortez, B. P. Dias Filho, *Rev. Bras. Farmacogn.* **2017**, *27*, 112–117.

[S11] C. Chepkirui, K.T. Yuyama, L. A. Wanga, C. Decock, J. C. Matasyoh, W. R. Abraham, M. Stadler, *J. Nat. Prod.* **2018**, *81*, 778–784.

[S12] Z. Rupcic, C. Chepkirui, M. Hernández-Restrepo, P. W. Crous, J. J. Luangsa-ard, M. Stadler, *Mycokeys* **2018**, *33*, 1–23.

[S13] G. Benny, Aliso **2008**, *26*, 37–61.